

Institute of Experimental and Clinical Pharmacology and Toxicology
Center for Experimental Medicine
University Medical Center Hamburg-Eppendorf
Director: Prof. Dr. med T. Eschenhagen

**Alterations of the ubiquitin-proteasome system
in targeted cMyBP-C mice
with hypertrophic cardiomyopathy**

Dissertation

submitted to the
Faculty of Medicine
University of Hamburg
for the degree
Doctor of Medicine

by

Daniel Riccardo Englmann

from Tübingen

Hamburg 2009

Accepted by the University of Hamburg: 29.09.2009

Published with the consent of the Faculty of Medicine
of the University of Hamburg

Examination board: Chairperson: Prof. Dr. T. Eschenhagen

Examination board: 2. Referee: PD Dr. S. Baldus

Examination board: 3. Referee: Prof. Dr. M. Glatzel

Table of contents

List of figures	V
List of tables	VI
1 Introduction	1
1.1 Heart structure and function	1
1.2 The sarcomere and cardiac myosin-binding protein C	2
1.3 Cardiac myosin-binding protein-C	5
1.4 Familial hypertrophic cardiomyopathy	5
1.5 The ubiquitin-proteasome system.....	8
1.6 Aim of the thesis.....	11
2 Material and Methods.....	12
2.1 Material.....	12
2.1.1 Animals.....	12
2.1.2 Chemicals	13
2.1.3 Chemicals with risk (R-) and safety (S-) phrases	15
2.1.4 Antibodies.....	16
2.1.5 Consumable material	17
2.1.6 Laboratory equipment.....	18
2.2 Methods	19
2.2.1 Protein preparation and determination of concentration	19
2.2.2 Western blot analysis.....	20
2.2.3 Chymotrypsin-like activity of the proteasome	22
2.2.4 Immunoprecipitation and tandem mass spectrometry	23
2.2.5 Statistical analysis	24
3 Results.....	25
3.1 Determination of the degree of cardiac hypertrophy.....	25
3.1.1 Investigation of KO mouse phenotype: heart weight and body weight ratio	25
3.1.2 Investigation of the mouse cardiac phenotype	25
3.1.3 Summary.....	27
3.2 Determination of calsequestrin amount in KO and WT mice	27
3.3 Determination of the steady-state levels of ubiquitinated proteins	28

3.3.1	Investigation of ubiquitinated proteins over age	29
3.3.2	Steady-state levels of ubiquitinated proteins at different post-natal time points	30
3.3.3	Investigation of specific ubiquitinated candidates.....	30
3.3.4	Summary.....	32
3.4	Investigation of protein degradation.....	33
3.4.1	Determination of the chymotrypsin-like activity in KO and WT mice.....	33
3.4.2	Determination of the levels of the β 5-subunit of the 20S proteasome	33
3.4.3	Investigation of ATP-depletion	36
3.4.4	Determination of the levels of pACC.....	38
3.4.5	Summary.....	39
3.5	Correlations	40
3.5.1	Correlation between ubiquitination and hypertrophy.....	40
3.5.2	Correlation between degradation and hypertrophy	40
3.5.3	Correlation between ubiquitination and degradation.....	41
3.5.4	Correlation between the amount and activity of the β 5-subunit.....	42
3.5.5	Correlation between degradation and ATP depletion.....	43
3.5.6	Summary.....	44
4	Discussion	45
4.1	Hypothesis 1: Cardiac hypertrophy results from the absence of cMyBP-C	46
4.2	Conclusion Hypothesis 1:.....	48
4.3	Hypothesis 2: High steady-state levels of ubiquitinated proteins result from impairment of the UPS.	49
4.4	Conclusion Hypothesis 2:.....	51
4.5	Hypothesis 3: A compensatory increase in the main degradation activity	51
4.6	Conclusion hypothesis 3:.....	52
4.7	Possible overview	52
4.8	Outlook.....	53
5	Abstract	55
6	Zusammenfassung	56
7	References	57
8	Appendix	66

8.1	Aminoacid Table	66
8.2	Mass spectrometry supplementary data.....	66
8.3	Tables.....	68
8.4	List of abbreviations	71
9	Acknowledgement.....	74
10	Curriculum Vitae.....	75
11	Declaration	76

List of figures

Figure 1.1: Electromechanical coupling of cardiomyocytes.....	2
Figure 1.2: The structure of the sarcomere.....	3
Figure 1.3: Muscle contraction by sliding of the myofilaments.....	4
Figure 1.4: Characteristics of hypertrophic cardiomyopathy.....	6
Figure 1.5: The two consequent steps of the ubiquitin proteasome system.....	8
Figure 1.6: Models of ubiquitin chain formation.....	9
Figure 2.1: Targeting strategy of the mouse MYBPC3 gene.....	12
Figure 2.2: Analysis of protein expression of cMyBP-C in WT and KO mice.....	13
Figure 2.3: Enzymatic reaction during degradation by the 20S proteasome.....	22
Figure 2.4: Substrate- and protein-dependent response of the chymotrypsin-like activity.....	23
Figure 3.1: Body and heart weights of WT and KO mice.....	25
Figure 3.2: Heart weight to body weight ratio in WT and KO.....	26
Figure 3.3: Evaluation of the profile of the level of CSQ during post-natal development.....	28
Figure 3.4: Evaluation of the levels of ubiquitinated proteins during post-natal development.....	29
Figure 3.5: Steady-state levels of ubiquitinated proteins in KO vs. WT at different post-natal ages.....	31
Figure 3.6: Comparison of band patterns after immunoprecipitation in WT and KO samples.....	32
Figure 3.7: Chymotrypsin-like activity of the proteasome in the KO and WT hearts.....	33
Figure 3.8: Evaluation of the profile of expression of the $\beta 5$ -subunit of the proteasome during post-natal development.....	34
Figure 3.9: Investigation of the $\beta 5$ -subunit levels in KO and WT mice.....	35
Figure 3.10: Enzymatic reaction following ATP-depletion.....	36
Figure 3.11: Evaluation of the profile of expression of pACC during post-natal development.....	37
Figure 3.12: Investigation of pACC in KO and WT mice.....	38
Figure 3.13: Correlation between the steady-state levels of ubiquitinated.....	40
Figure 3.14: Correlation between the chymotrypsin-like activity and the.....	41
Figure 3.15: Correlation between the steady-state levels of ubiquitinated.....	42
Figure 3.16: Correlation between the steady-state levels of $\beta 5$ -subunit.....	43
Figure 3.17: Correlation between ATP-depletion and degradation.....	44
Figure 4.1: A model of the pathomechanism of hypertrophic cardiomyopathy.....	53

List of tables

Table 1.1:	Sarcomeric genes and mutations involved in FHC.....	7
Table 2.1:	Antibodies used for protein analysis in tissue.....	21
Table 3.1:	Percentage of change of the HW/BW ratio in KO relative to WT.....	27
Table 8.1:	Identificaion of desmin by peptide sequence.....	66
Table 8.2:	Identification of amino acid sequence belonging to a peptid of desmin.....	67
Table 8.3:	Raw data WT and KO NN.....	68
Table 8.4:	Raw data WT and KO 2wks.....	68
Table 8.5:	Raw data WT and KO 4wks.....	69
Table 8.6:	Raw data WT and KO 6wks.....	69
Table 8.7:	Raw data WT and KO 9wks.....	70
Table 8.8:	Raw data WT and KO 13wks.....	70
Table 8.9:	Raw data WT and KO 50wks.....	71

1 Introduction

“A protein’s life within the cell is likely to be nasty, brutish and short” (Goldberg 2003).

In the year of 2004 the Nobel Prize in chemistry was given by The Royal Swedish Academy of Sciences to three scientists: Aaron Ciechanover, Avram Hershko and Irwin Rose “for the discovery of ubiquitin-mediated protein degradation”. Since then more and more publications have indicated that this complex cellular system is altered in many neurodegenerative pathologies (Lim and Tan 2007). In cardiovascular research there is still a lack of knowledge. How could this vital system be involved in hypertrophic cardiomyopathy, which is one of the most frequent cardiac diseases?

1.1 Heart structure and function

The heart provides with its repeated rhythmic contractions the pumping capacity to hold up blood circulation. The heart-specific muscle shows characteristics of both striated muscle and smooth muscle cells and generates a huge pumping force with a big endurance. In an average life time taking into account only its work at rest, it pumps approximately 159 million liters of blood (Cabin 1992). This volume is equivalent to the load of 3.3 super tankers. During exercise or stress the heart may increase its pumping capacity up to 10 times. Cardiomyocytes intercommunicate through gap junctions, of which one function is to propagate action potentials (Uhlir 2005). The heart works as a single unit muscle recruiting and stimulating all myocytes at once. The electromechanical coupling of the contraction-relaxation cycle is shown in Figure 1.1. In cardiac myocytes a voltage-dependent Ca^{2+} channel is located in the sarcolemma (Silbernagl and Despopoulos 2007). After action potential activation a small amount of extracellular Ca^{2+} enters the cell through this channel. It triggers a conformational change of the ryanodine receptors of type 2 located in the sarcoplasmic reticulum (SR) to open this Ca^{2+} -dependent Ca^{2+} channel. Consecutively a great amount of Ca^{2+} ions of the SR is released. This boosting effect enables the contraction during systole. For relaxation during diastole the additional Ca^{2+} is pumped out of the cell and reuptaken by the SR. The contraction will be explained in detail in the next chapter.

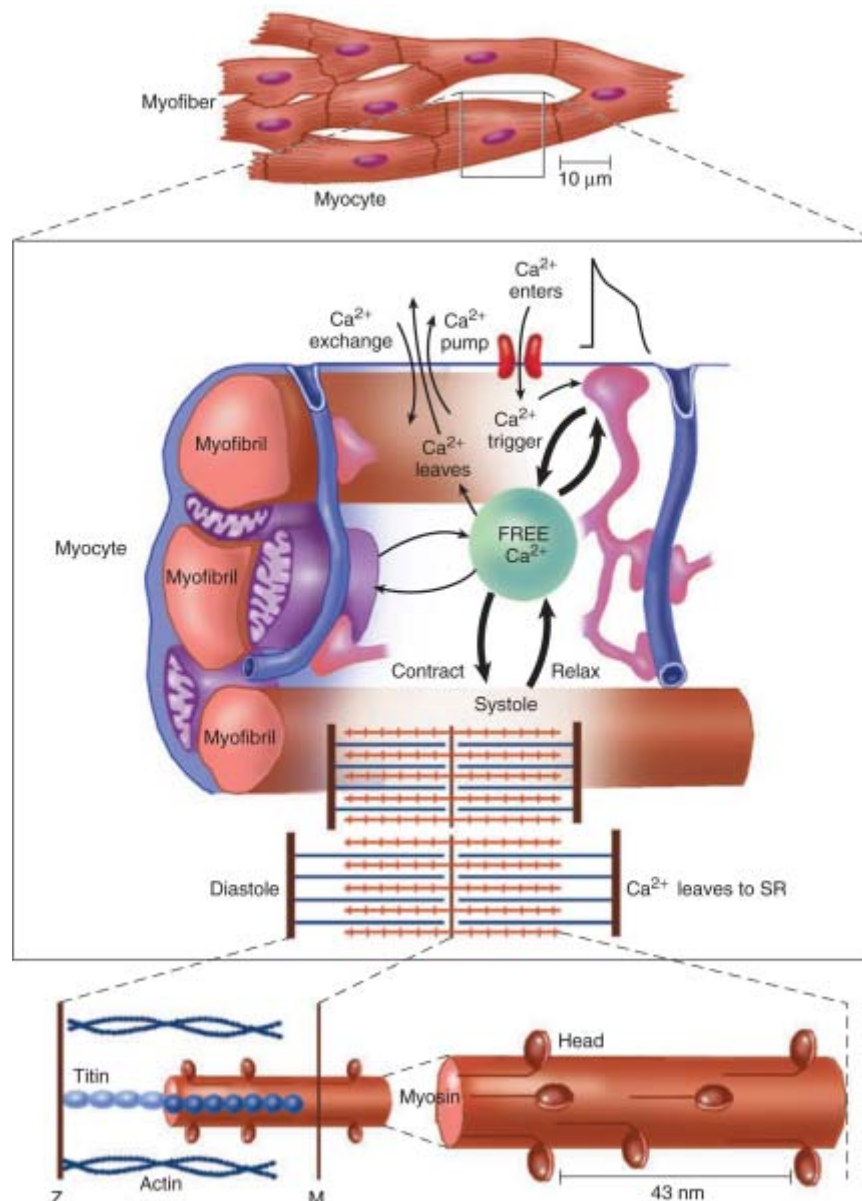


Figure 1.1: Electromechanical coupling of cardiomyocytes.

Upper panel, shows a schematic myofiber composed of myocytes. **Middle and lower panels,** an action potential travelling along the sarcolemma activates the dihydropyridine receptor (Ca^{2+} channel) and Ca^{2+} ions enter the myocyte. These Ca^{2+} ions trigger the release of more calcium from the sarcoplasmic reticulum and thereby initiate contraction. Eventually, the small amount of calcium that has entered the cell will leave predominantly by a $\text{Na}^+/\text{Ca}^{2+}$ exchanger and with a lesser role for the sarcolemmal calcium pump. The varying actin-myosin overlap during the contraction-relaxation cycle is shown for the systole, when calcium ions arrive, and the diastole, when calcium ions leave. The myosin heads of the thick filaments interact with the thin filaments (adapted from Opie and Solaro 2004 and Braunwald et al., 1976).

1.2 The sarcomere and cardiac myosin-binding protein C

Every myofibril is divided by the so called Z-lines into sarcomeres. Sarcomeres consist of three filament-systems: The thick one mainly composed of myosin II molecules, from which every one is constituted of two regulatory light chains and two heavy chains, which

bind to the thin actin filament. The thin filament-system is made up of actin, which forms two intertwining helical chains (G-actin and F-actin) and regulatory proteins such as tropomyosin and the troponin complex (Brenner 2005). The titin-filament-system is the third filament-system, which connects the M- (which is in the middle between two Z-lines) and the Z-line holding the thick filament in place (Silbernagl and Despopoulos 2007). In Figure 1.2 the sarcomere is schematically presented.

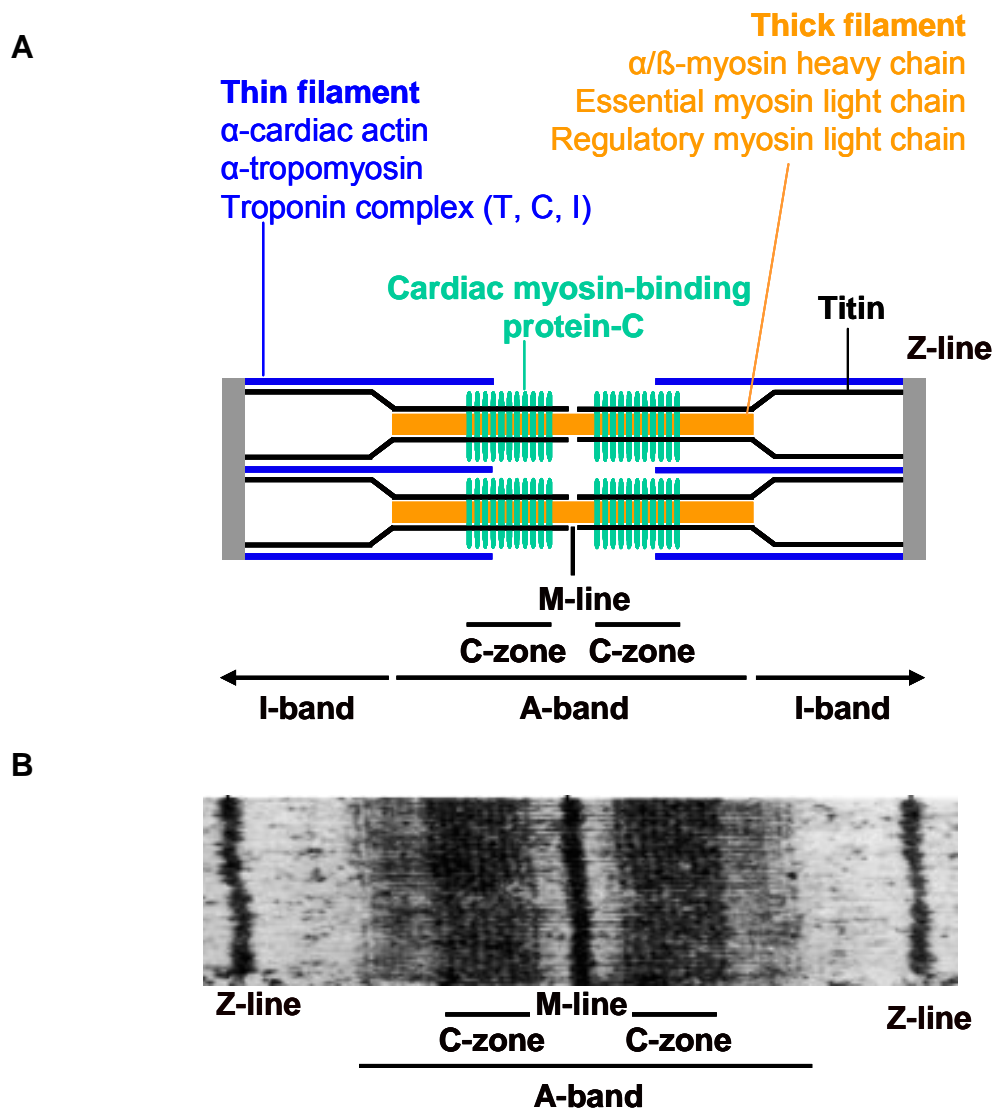


Figure 1.2: The structure of the sarcomere.

A, Schematic structure of the sarcomere (adapted from Bonne et al., 1998). **B**, Electron microscopical picture of the sarcomere (adapted from Craig and Offer 1976).

Viewed through the light microscope the sarcomere has an alternating lighter and darker appearance of bands and lines producing the typical striation image of filaments (Figure 1.2B). The darker bands, which mainly consist of myosin filaments, are in the polarized

light birefringent. They are called A-bands (from anisotropic). On each side of the M-line every A-band has a C-zone. The I-band (from isotropic) is less birefringent; it is mainly made up of actin and lies between two A-bands. In the C-zones of the A-bands the sarcomeric cardiac myosin binding protein C (cMyBP-C) is localized (Offer et al., 1973).

The sarcomere is the contractile unit of the muscle. Although the length of the muscle alters during tension, there is no change of the end to end distance of the thick and the thin filament, suggesting that they slide against each other during contraction and relaxation (Figure 1.1). This sliding is inhibited by tropomyosin, which overlays the binding sites of actin on myosin in the resting muscle (Figure 1.3). The troponin-complex regulates the conformational changes of tropomyosin. It has three subunits, with its troponin-T subunit (T for tropomyosin binding) and with the troponin-I subunit (I for inhibitory) the tropomyosin is hold in place. In the relaxed muscle only two of the four binding sites for Ca^{2+} of troponin C (for Ca^{2+}) are occupied. When it binds to two more Ca^{2+} ions the conformational change of the troponin-complex is induced, activating the movement of tropomyosin and liberating the binding site for myosin on actin. ATP can bind to the motor protein myosin and the energy released by hydrolyzing ATP is used to facilitate conformational changes in myosin, which therefore slides along the actin filaments. The muscle relaxes when Ca^{2+} is pumped back into the SR and tropomyosin reblocks the binding sites for myosin on actin (Brenner 2005).

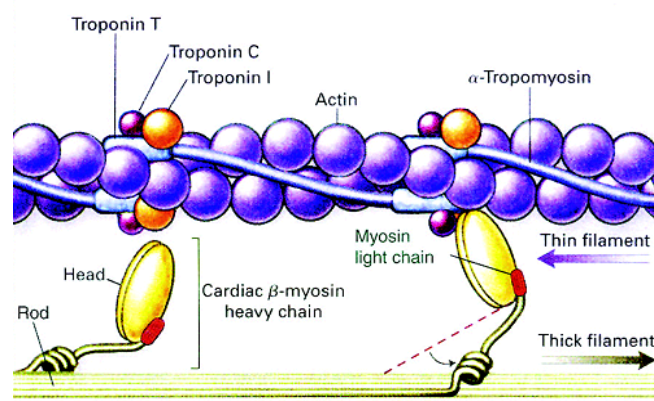


Figure 1.3: Muscle contraction by sliding of the myofilaments.

Contraction begins with Ca^{2+} binding to troponin C, which induces a conformational change of the troponin-complex that subsequently leads to actin-myosin interaction. ATP is then hydrolyzed by myosin, and the thick filaments are displaced along the thin filaments. As Ca^{2+} is sequestered by the sarcoplasmic reticulum, actin-myosin interactions are prevented (adapted from Kamisago et al., 2000).

1.3 Cardiac myosin-binding protein-C

Myosin-binding protein-C (MyBP-C) was first described by Offer and co-workers in 1973 (Offer et al., 1973). It has a molecular weight of 140 to 150 kDa and is localized in the cross-bridge bearing region (C-zone) of the A-band (Figure 1.2). This zone contains a set of eleven transverse repeats distributed along the constant diameter section of the thick filament, from which seven to nine of these repeats are recognized by antibodies directed against MyBP-C. It belongs to the intracellular immunoglobulin superfamily and there are three isoforms of MyBP-C: the slow-skeletal, the fast-skeletal and the cardiac isoform (Freiburg and Gautel 1996; Alyonycheva et al., 1997). The amount of MyBP-C is of about 2% in the myofibril (Offer et al., 1973). It might play a structural role by stabilizing the thick filament via its interactions with myosin, actin and titin. Moreover there is evidence that MyBP-C has a regulatory role by affecting the potentials of interaction between myosin and actin (Flashman et al., 2004). The gene encoding cMyBP-C is *MYBPC3* (Carrier et al., 1997).

1.4 Familial hypertrophic cardiomyopathy

Hypertrophic cardiomyopathy (HCM) is characterized by asymmetrical septal hypertrophy (considered pathologic in humans when more than 13 mm depth) and thickened left ventricular walls (Figure 1.4). HCM is often associated with interstitial fibrosis (Richardson et al., 1996). It is a relatively frequent disease with a prevalence of 1:500 in the general population and is the most common cardiovascular disease in many countries (Maron et al., 1995). HCM is an important cause of disability and death. Unfortunately it is still the most frequent cause of sudden death in young athletes during exercise. Most patients have none or only minor symptoms. HCM should be suspected when the following features like heart murmurs, a positive family history, new heart associated symptoms or electrocardiogram (ECG) alterations appear in a patient. Nevertheless most of these signs are only detected in patients with hypertrophic obstructive cardiomyopathy (HOCM), which represent 25% of the HCM patients. Thus, the facultative symptoms are vertigo, chest pain, syncope and dyspnea. HCM may result in heart failure, malignant arrhythmia and sudden death (for reviews, see Maron et al., 1999; Maron 2002). In about 70% of cases HCM is familial (FHC; for review, see Richard et al., 2006).

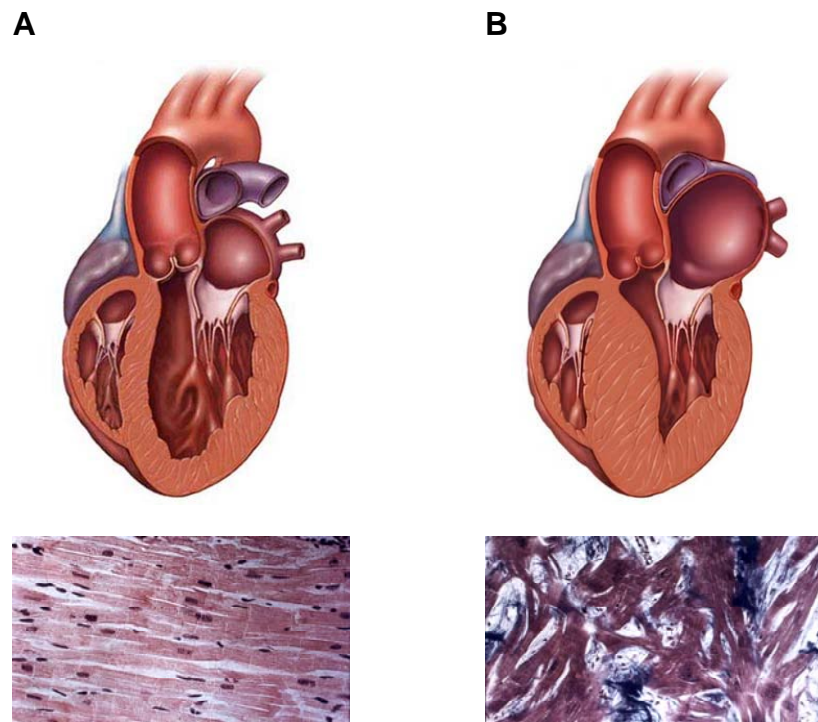


Figure 1.4: Characteristics of hypertrophic cardiomyopathy.

A, On the top, a schematic longitudinal cardiac section of a healthy heart is shown. Below, the histology of a healthy cardiac section stained with Sirius Red is presented. **B**, On the top, a schematic longitudinal cardiac section of a hypertrophied heart is shown. The walls of the left ventricle are thickened. Below the histological image shows hypertrophied cardiomyocytes, which lost their parallel arrangement. Additionally interstitial fibrosis (in blue) was found after staining with Sirius Red (adapted from the Mayo Clinic website and from Geisterfer-Lowrance et al., 1990).

FHC is an autosomal dominant disease of the cardiac sarcomere, caused by more than 400 mutations in at least 13 genes that encode different components of the contractile apparatus (Table 1.1; Alcalai et al., 2008). Carrier and co-workers identified the *CMH4* locus on chromosome 11 in 1993 (Carrier et al., 1993) and the first mutation in *MYBPC3* in 1995 (Bonne et al., 1995). Mutations in *MYBPC3* are frequently involved in FHC (Richard et al., 2003). The two most frequently mutated genes involved are *MYH7* (44%) encoding β -myosin heavy-chain and *MYBPC3* (34%) encoding cMyBP-C (for reviews, see Richard et al., 2006; Alcalai et al., 2008).

FHC gene	Symbol	Mutations
β -myosin heavy chain	<i>MYH7</i>	212
Myosin-binding protein-C	<i>MYBPC3</i>	165
Troponin T	<i>TNNT2</i>	33
Troponin I	<i>TNNI3</i>	27
Alpha-tropomyosin	<i>TPM1</i>	12
Regulatory myosin light chain	<i>MYL2</i>	10
Actin	<i>ACTC1</i>	7
Essential myosin light chain	<i>MYL3</i>	5
Titin	<i>TTN</i>	2
Muscle LIM protein	<i>CSRP3</i>	3
Telethonin	<i>TCAP</i>	2
Cardiac troponin C	<i>TNNC1</i>	1
Alpha-myosin heavy chain	<i>MYH6</i>	1

Table 1.1: Sarcomeric genes and mutations involved in FHC.

Table was adapted from Alcalai et al. (2008) and Richard et al (2006).

Most mutations (70%) found in *MYBPC3* are frameshift or nonsense mutations (Richard et al., 2006; Alcalai et al., 2008). These mutations should produce C-terminal truncated proteins, because of premature appearance of stop codons in the mRNA transcript. However, up to now it was not possible to detect them in human hearts (Rottbauer et al., 1997; Moolman et al., 2000; Van Dijk et al., 2009). In contrast, the mutant proteins encoded by missense mutations are stable and could be detected in mouse models and in human soleus muscle (Cuda et al., 1993; Bottinelli et al., 1998).

Currently two molecular mechanisms are hypothesized to lead to FHC. In the “poison peptide theory” it is assumed that the mutant proteins exert adverse effects on the structure/function of the sarcomere. The other hypothesis is that the mutant allele acts as a null allele leading to a reduction (“haploinsufficiency”) of the wild-type cMyBP-C amount in the sarcomere (Yang et al., 1998; Carrier et al., 2004). The stoichiometric imbalance between the thick filament components could result in alterations in the structure and function of the sarcomere and subsequently in FHC. Two recent papers strongly suggest that the ubiquitin-proteasome system (UPS) is responsible of the instability of the truncated protein. Thus, a truncated cMyBP-C resulting from a human mutation, after gene transfer in cardiomyocytes, was rapidly and quantitatively degraded by UPS (Sarikas et al., 2005; Bahrudin et al., 2008). This data showed for the first time that involvement of the UPS

could be responsible for protein instability in FHC patients.

1.5 The ubiquitin-proteasome system

In a highly selective dynamic process proteins are continually degraded to amino acids and resynthesized (for review, see Goldberg 2003). Damaged proteins are harmful to cells, because they are able to activate apoptotic pathways, they can aggregate and produce other gain-of-function toxicities (Patterson et al., 2007). Not only in pathological circumstances damaged or misfolded proteins can arise, but also under physiological conditions a large amount of the *de novo* synthesized proteins are rapidly degraded (for review, see Goldberg 2003). Of all cell organelles the lysosomes and proteasomes provide the main proteolytic activities. The function of the lysosomes consists in the destruction of endocytosed surface proteins.

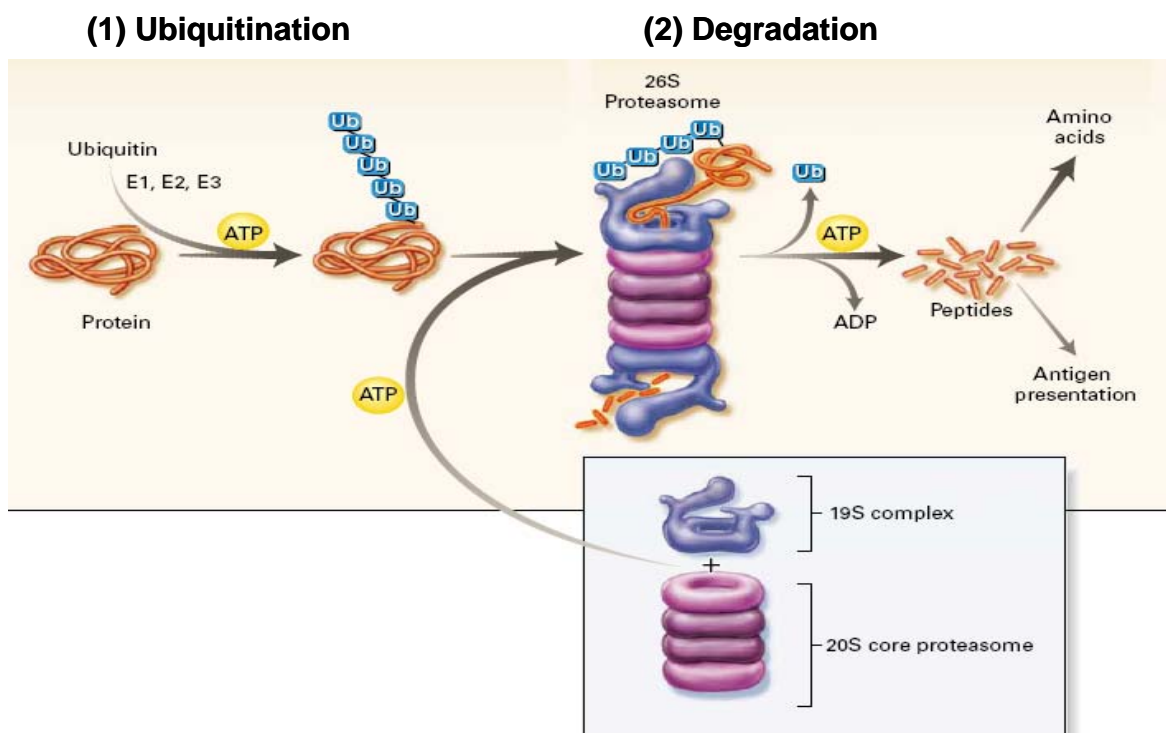


Figure 1.5: The two consequent steps of the ubiquitin proteasome system.

On the left part the ATP-dependent process of ubiquitination is shown. It is a multi-step process in which three enzymes are involved. The right part illustrates the degradation by the 26S proteasome complex, which consists of the 20S core and the 19S lid. The ubiquitin-tagged proteins enter the proteasome and are then degraded by the two inner β -rings which are surrounded by the two outer α -rings (as shown in the lower part). Thereafter the peptides and ubiquitin are released. The de-ubiquitinating enzymes are not shown (adapted from Mitch and Goldberg 1996).

In contrast the UPS is a quality-control system in eukaryotic cells responsible for the degradation of most intracellular proteins. Moreover it has been shown that this system is involved in intracellular signalling, transcriptional control or regulation of cell death. The majority of proteins destined for degradation are covalently linked in a three-step-cascade process to poly-ubiquitin (for reviews, see Zolk et al., 2006; Mearini et al., 2008). Ubiquitin is a 76 amino acid protein, which shows an evolutionary high conservative amino acid sequence (Hershko and Ciechanover 1982). Figure 1.5 shows the steps of ubiquitination and degradation of the UPS pathway. The process of ubiquitination is carried out by at least three enzymes (E1, E2 and E3). The process starts with E1 (ubiquitin-activating enzyme). In the second, intermediate step the activated ubiquitin is covalently linked in an ATP-dependent reaction to E2 (ubiquitin-conjugating enzyme). In the last step ubiquitin is either directly conjugated from E2 to the substrate in which E3 acts as a bridging factor or indirectly whereas some E3 ligases form an ubiquitin-thio-ester intermediate before transferring ubiquitin to the protein (for review Mearini et al., 2008). The ubiquitin chain is then elongated to tag proteins for their final destination. Depending on the number of ubiquitin molecules the aims are different. Surface proteins linked to one ubiquitin are internalized. In contrast intracellular proteins with an ubiquitin chain of four or more are digested by the proteasome (for review, see Mearini et al., 2008; Figure 1.6). Most of these proteins are misfolded and/or damaged (for review, see Goldberg 2003).

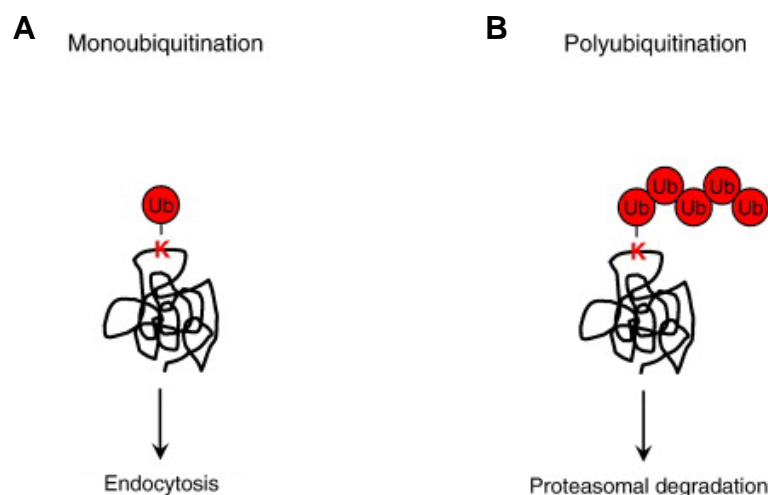


Figure 1.6: Models of ubiquitin chain formation.

A Proteins linked to a single ubiquitin lead to endocytosis. **B** Polyubiquitinated proteins are recognized for UPS-mediated degradation. (adapted from Mearini et al., 2008).

The 26S proteasome is an organelle usually consisting of three parts (for review, see Mearini et al., 2008). It offers two regulatory 19S and a catalytic 20S core subunit (core particle). The core particle consists of four heptametrical layers: two identical inner β -rings and two identical α -outer rings. Each of them consists of seven different subunits. The catalytic activities are localized to some of the β -subunits. The main catalytic site is the $\beta 5$ -subunit that provides the chymotrypsin-like activity. In addition there are two other proteolytic activities, the trypsin-like in the $\beta 2$ subunit and the caspase-like in the $\beta 1$ subunit. Inside the inner rings the protein is cut into peptides. The base of the 19S proteasome is built up of nine subunits, of which six have ATPase activity. The function of the lid still remains unclear. The 19S proteasome recognizes ubiquitin-tagged proteins and regulates the entry to the 20S core particle. Due to a narrow orifice it was hypothesized that proteins are unfolded and the 19S proteasome makes access available. After being degraded short peptides of the initial substrate and reusable ubiquitin are released. The single ubiquitin molecules are separated by de-ubiquitinating enzymes (DUBs; for review, see Ciechanover 2006).

A large body of evidence indicates UPS alterations in human or experimental cardiac disease (for review, see Mearini et al., 2008). Whereas accumulation of ubiquitinated proteins is a common feature of cardiac disease and suggests UPS impairment, the activities of the proteasome are not consistently depressed in affected hearts. Similarly, the expression of the UPS components such as E2 conjugating-enzymes, E3 ubiquitin ligases, or subunits of the proteasome are either increased or decreased in cardiac disease.

Specifically, cardiac hypertrophy occurs as an adaptive response to increased workload to maintain cardiac function in response to physiological or pathological stress. While physiological hypertrophy can result from exercise, pathological hypertrophy responds to events such as volume or pressure overload, ischemia, or genetic abnormalities. Prolonged pathologic cardiac hypertrophy causes heart failure, and its mechanisms are largely unknown. Cardiac remodeling during hypertrophy and failure involves global increase in gene expression, including re-expression of fetal genes such as β -MHC and α -skeletal actin, or up-regulation of the expression of atrial/brain natriuretic factors (for reviews, see Boheler et al., 1991; Schwartz et al., 1992). One key element of cardiac hypertrophy is an adaptation in protein turnover. It refers to both protein synthesis and degradation, and interestingly, while synthesis has always been shown to be stimulated, protein degradation was either accelerated or unchanged in hypertrophic hearts, but inhibited by induction of

cardiac work or high aortic pressure in Langendorff preparations (Gordon et al., 1987; Morgan et al., 1987). More recently, accumulation of ubiquitinated proteins has been reported in human heart failure (Hein et al., 2003; Weekes et al., 2003) suggesting impaired UPS. In an experimental mouse model of heart failure induced by transverse aortic constriction (TAC) both increased steady-state levels of ubiquitinated proteins and depression of proteasome activities were observed (Tsukamoto et al., 2006). These lines of evidence are consistent with the hypothesis that removal of abnormal proteins by the proteasome is insufficient in heart failure. However, depressed UPS was not detected consistently and recent data rather showed an activation of the UPS, including increased levels of UPS components and proteasome activities in murine, canine and feline models of TAC-induced cardiac hypertrophy (Balasubramanian et al., 2006; Depre et al., 2006). However, no investigations were performed in engineered mice with cardiac hypertrophy.

1.6 Aim of the thesis

The aim of my work was therefore to investigate whether alterations of the UPS are found in an engineered mouse model exhibiting cardiac hypertrophy. The mouse model is deficient in cMyBP-C (cMyBP-C-KO; Carrier et al., 2004).

Three hypotheses were investigated:

1. Cardiac hypertrophy results from the absence of cMyBP-C and is associated with high steady-state levels of ubiquitinated proteins.
2. High steady-state levels of ubiquitinated proteins result from impairment of the UPS.
3. UPS impairment leads to misusage of ATP.

2 Material and Methods

2.1 Material

2.1.1 Animals

The investigations conform with the guide for the care and use of laboratory animals published by the NIH (Publication No. 85-23, revised 1985).

2.1.1.1 The cMyBP-C knock-out mouse model

The cMyBP-C-KO (KO) mouse model, developed by Lucie Carrier in Paris, is a transcriptional knock-out (Carrier et al., 2004). The genetic background was blackswiss. It was generated by targeted deletion of exons 1 and 2 which included the transcription initiation site of the mouse *MYBPC3* gene by a neo cassette (Figure 2.1). In homozygous KO mice, neither cMyBP-C mRNA nor protein were detected, validating the gene inactivation. These mice develop eccentric left ventricular (LV) hypertrophy with decreased fractional shortening and a significant increase of the LV mass to body weight

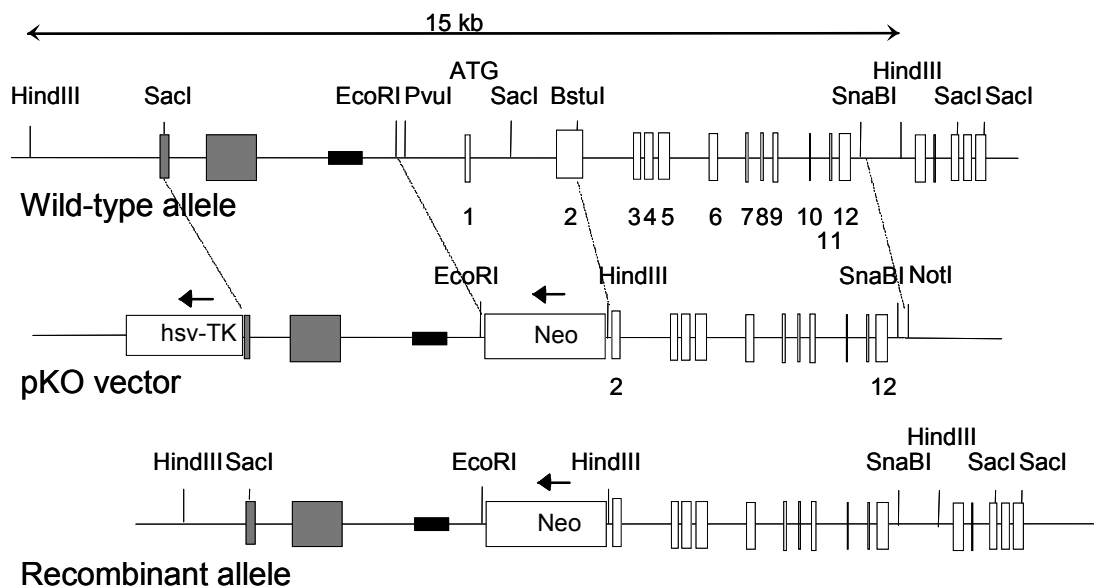


Figure 2.1: Targeting strategy of the mouse *MYBPC3* gene.

The genomic region of interest of *MYBPC3* with the ATG starting site is shown on the top, the pKO targeting construct is shown in the center, and the mutated locus after homologous recombination is shown at the bottom (from Carrier et al., 2004).

ratio at the age of 3-4 months compared to corresponding wild-type littermates. In addition, histological examination at this age showed myocardial disarray, increased interstitial fibrosis and calcification in the fibrotic areas. To confirm first that KO animals in Hamburg do not express any cMyBP-C we performed a Western blot analysis with an antibody directed against cMyBP-C. Figure 2.2 clearly shows the absence of cMyBP-C in the KO mice from neonates (NN) to 9 wks.

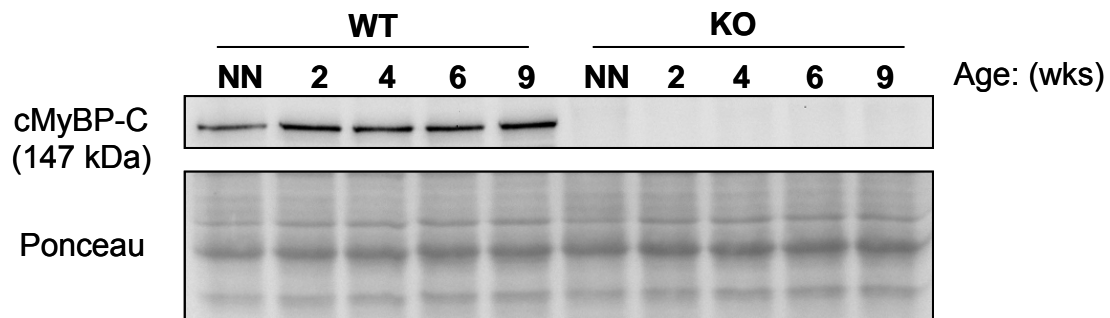


Figure 2.2: Analysis of protein expression of cMyBP-C in WT and KO mice.

The ventricular proteins of 8 gender matched animals were pooled for each time point. The blot was stained with an antibody directed against cMyBP-C. Below the blot the corresponding Ponceau is shown. Abbreviations used are: NN, neo-nates; KO, cMyBP-C knock-out mice; WT, cMyBP-C wild-type mice.

2.1.1.2 Mouse cardiac phenotype

To analyze the cardiac phenotype in both mouse groups, the heart-weight-to-body-weight ratio (HW/BW) was calculated. The mice were sacrificed by cervical dislocation in light CO₂ anaesthesia and weighted. After preparation of the hearts, the cardiac weights were determined; tissues were frozen in liquid nitrogen and stored at -80 C until utilisation. The HW/BW ratios were determined and calculations were performed with the GraphPad Prism4 (GraphPad Software, Inc.) software.

2.1.2 Chemicals

Product	Company
Acetone	Merck®
Acrylamide/bis solution (29:1)	Bio-Rad®

Product	Company
Adenosine 5'-triphosphate (ATP)	Sigma [®]
Ammonium persulfate (APS)	Bio-Rad [®]
Aqua ad injectabilia	Baxter GmbH [®]
Bovine serum albumin (BSA)	Sigma [®]
Bromophenol blue	Merck [®]
Complete mini-proteases inhibitor cocktail	Roche Diagnostics [®]
Coomassie Brilliant Blue G-250 reagent	Bio-Rad [®]
Dimethyl sulfoxide (DMSO)	Sigma [®]
Dithiothreitol (DTT)	Sigma [®]
Ethidium bromide	Fluka [®]
Ethylenediaminetetraacetic acid (EDTA)	Sigma [®]
Glycerol	Merck [®]
Glycine	Roth [®]
Hydrochloric acid (HCl)	Merck [®]
Immunoglobulin G	Sigma [®]
Isotonic 0.9% sodium chloride solution	Baxter GmbH [®]
L-glutamine	Gibco [®]
Loading dye, 6x	Fermen [®] tas
Magnesium acetate tetrahydrate (Mg(CH ₃ COO) ₂ ·4H ₂ O)	Merck [®]
Magnesium chloride hexahydrate (MgCl ₂ ·6H ₂ O)	Roth [®]
Methanol	J. T. Baker [®]
Milk powder	Roth [®]
Phosphate buffered saline (PBS)	Biochrom [®]
Phosphocreatine	Calbiochem [®]
Phosphocreatinekinase	Sigma [®]
Ponceau S	Serva [®]
Potassium chloride (KCl)	Merck [®]
Precision Plus Protein Standard™	Bio-Rad [®]

Product	Company
Sodium chloride (NaCl)	J. T. Baker [®]
Sodium dodecyl sulfate (SDS)	Roth [®]
Sodium fluoride (NaF)	Merck [®]
Sodium hydrogen carbonate (NaHCO ₃)	Merck [®]
Sodium hydroxide (NaOH)	Merck [®]
Succinyl-leucyl-leucyl-valyl-tyrosyl-7-amino-methylcoumarin (SUC-Leu-Leu-Val-Tyr-AMC)	Calbiochem [®]
SuperSignal [®] West Dura extended duration substrate	Pierce [®]
Tetramethylethylenediamine (TEMED)	Bio-Rad [®]
Trishydroxymethylaminomethane (Tris) base	Sigma [®]
Tris hydrochloride (Tris-HCl)	Promega [®]
Triton X-100	Sigma [®]
Polyoxyethylene (20) sorbitan monolaurate (Tween [®] 20)	Sigma [®]

2.1.3 Chemicals with risk (R-) and safety (S-) phrases

Acetone	R: 11-36-66-67	S: 9-16-26
Acrylamide/bis solution	R: 23/24/25-45-46-48	S: 36/37/39-45-60
ATP	R: -	S:22-24/25
APS	R: 8-22-36/37/38-42/43	S: 22-24-26-37
Bromphenol blue	R: -	S:22-24/25
Coomassie Brilliant Blue G-250 reagent	R: 20/21/22-34-68	S: 26-36/37/39-45
DMSO	R: 36/37/38	S: 23-26-36
DTT	R: 22-36/37/38	S: 26-36
Ethidium bromide	R: 23-68	S: 36/37-45
EDTA	R: 36-52/53	S: 26-61
Glycine	R: -	S: 22-24/25

Magnesium acetate tetrahydrate	R: -	S: 22-24/25
Sodium chloride (NaCl)	R: 11-23/24/25-39	S: 7-16-36/37-45
PBS	R: -	S: 22-24/25
Ponceau S	R: 36/37/38-51/53	S: 2-25-26-29/56-37-46-57-60-64
Potassium chloride	R: -	S: 22-24/25
SDS	R: 22-36/38	S: 22-24/25
Sodium fluoride	R: 25-32-36/38	S: 22-36-45
Sodium hydroxide	R: 35	S: 26-37/39-45
TEMED	R: 11-20/22-34	S: 16-26-36/37/39-45-60
Tris base	R: 36/37/38	S: 26-36
Tris hydrochloride	R: 36/37/38	S: 26-36
Triton X-100	R: 22-41-51/53	S: 26-36/39-61

2.1.4 Antibodies

Anti- β 5	Wang, University of South Dakota, Sioux Fall, SD
Anti-cMyBP-C	Linke, University of Heidelberg
Anti-Calsequestrin (PA1-913)	Dianova [®]
Anti-mouse IgG peroxidase conjugate	Dianova [®]
Anti-rabbit IgG peroxidase conjugate	Sigma [®] and Dianova [®]
Anti-phospho-acetyl CoA Carboxylase (07-303)	Upstate [®]
Anti-ubiquitinated proteins (clone FK2, PW-8810)	Biomol [®]
Anti-ubiquitin (P4D1), monoclonal	Santa Cruz Biotechnology [®]

2.1.5 Consumable material

Product	Company
Blotting paper (Whatman 3MM)	Schleicher & Schuell [®]
Cuvettes (10 x 4 x 45 mm)	Sarstedt AG & Co. [®]
Falcon tubes (15 and 50 ml)	Sarstedt AG & Co. [®]
Hypodermic needles (Sterican [®] Gr.20)	Braun [®]
Lab-Tek [™] chambers	Nalge Nunc International [®]
Latex gloves	Paul Hartmann AG [®]
Micro tubes (1.5, 2.0 ml)	Sarstedt AG & Co. [®]
Multiple well plate (96-well)	Sarstedt AG & Co. [®]
Nitrile gloves	Ansell [®]
Nitrocellulose membrane (Protran [®] BA 85)	Schleicher & Schuell [®]
Nylon membrane (Hybond N+)	Amersham Biosciences [®]
Pipette tips (for 10, 100 and 1000 µl pipettes)	Sarstedt AG & Co. [®]
Serological pipettes (2, 5, 10 and 25 ml)	Sarstedt AG & Co. [®]
Serological pipettes (10 ml, wide tip)	Becton Dickinson [®]
Sterile filter (0.22 µm)	Sarstedt AG & Co. [®]

2.1.6 Laboratory equipment

Product	Company
Accu-jet pipetting aid	Brand GmbH [®]
Analytical balance (GENIUS)	Sartorius AG [®]
Benchtop centrifuge	Sarstedt AG & Co. [®]
Blotting system (Mini Trans-Blot [®] cell)	Bio-Rad [®]
Centrifuge (5810 R)	Eppendorf AG [®]
Chemie Genius ² Bio imaging system with Gene Tools software	Syngene [®]
Electrophoresis system (Mini PROTEAN [®] 3 electrophoresis cell)	Bio-Rad [®]
Ice machine	Scotsman [®]
Magnetic stirrer (IKAMAG [®] RCT)	Janke & Kunkel GmbH [®]
Microplate reader (Tecan Safire ²)	Tecan [®]
Microcentrifuge (5415 R)	Eppendorf AG [®]
Microwave	Sharp [®]
Neubauer chamber	Glaswarenfabrik Karl Hecht KG [®]
pH-meter	Knick GmbH [®]
Pipettes (10, 100, 1000 µl)	Eppendorf AG [®]
Portable balance (Scout [™] Pro)	Ohaus [®]
Power supply	Bio-Rad [®]
Precision balance (Precision Advanced)	Ohaus [®]
Rectal thermometer	Physitemp [®]
Spectrophotometer (Smart Spec [™] 3000)	Bio-Rad [®]
Surgical instruments	Karl Hammacher GmbH [®]
Tissue Lyser	Qiagen [®]
Thermomixer comfort	Eppendorf AG [®]
Ultra-pure water system Milli-Q plus	Millipore [®]

Product	Company
Vortexer (Vibrofix VF1)	Janke & Kunkel GmbH [®]
Water bath	GFL [®]

2.2 Methods

2.2.1 Protein preparation and determination of concentration

Frozen hearts were powdered with a steel mortar in liquid nitrogen. The powder was divided in three safe-lock Eppendorf[®] tubes –for protein extraction either for Western blot, chymotrypsin-like activity measurements or immunoprecipitation.

Tissue samples for whole tissue protein extraction for subsequent Western blot analysis were weighted, mixed with 10 volumes of lysis buffer I (3% SDS, 30 mM Tris base, pH 8.8, 5 mM EDTA, 30 mM NaF, 10% glycerol) and homogenized with the Tissue Lyser (Qiagen[®]) 60 sec at a frequency of 30 Hz. Protein concentration for Western blot analysis was determined by the Lowry protein assay (Bradford 1976). This method is a fast and simple spectroscopic analytical procedure used to measure the concentration of proteins in a solution. Proteins react with cupric sulphate and tartrate in an alkaline solution, which results in formation of tetradentate copper-protein complexes. By adding the Folin-Ciocalciu Reagent (PIERCE[®]), it is reduced in portion to the chelated complexes mentioned before, producing a blue coloured product which can be measured at 750 nm. First a standard curve of the absorbance versus micrograms protein was prepared. To this end diluted albumin standards (BSA) were used in a range of 0 to 1500 µg/ml. Protein concentration of unknown samples was then calculated by comparison with the standard curve. All protein samples were diluted 1:40 in distilled water prior measurement to ensure that their obtained values were within the range of standard curve. For measurements the Modified Lowry Protein Assay Kit from PIERCE[®] was used.

For measurement of the 20S proteasome activities, about 30-50 mg tissue powder were mixed with five volumes of lysis buffer III (1 tablet complete mini-proteases inhibitor cocktail dissolved in 10 ml aqua ad iniectabilia) to extract the cytosolic fraction. After three cycles of freezing (in liquid nitrogen) and thawing (at room temperature) the samples were

homogenized with the Tissue Lyser as described above. After centrifugation (13200 rpm, 30 min, 4 °C), the supernatant was collected. The protein concentration of the supernatant was then determined by the Bradford protein assay, which is a dye-binding assay in which a differential color change of a dye occurs in response to various concentrations of protein (Bradford 1976). For determination, 5 µl of supernatant of protein samples were added to 795 µl of 0.1 M NaOH. After admixture of 200 µl Coomassie Brilliant Blue G-250 reagent and incubation at room temperature for 5 min, the absorbance at 595 nm was measured with a spectrophotometer. Subtraction of the blank value (800 µl of 0.1 M NaOH plus 200 µl Coomassie Brilliant Blue G-250 reagent) and comparison to a standard (immunoglobulin G) curve provided a relative measurement of protein concentration. Each protein concentration determination was performed in duplicates.

For immunoprecipitation, proteins were extracted with 10 volumes of RIPA high salt buffer (500 mM NaCl, 1 mM EDTA, 50 mM Tris HCl pH 7.4, 1% Triton; for protease inhibitor –1 tablet of Complete Mini, Roche[®] for 10 ml buffer was used) and homogenized with the Tissue Lyser (Qiagen[®]) 60 sec at a frequency of 30 Hz. For protein concentration the Bradford protein assay as described above was used.

2.2.2 Western blot analysis

For Western blot analysis 10 µg (tissue) of protein were adjusted to Laemmli buffer composition (2% SDS, 10% glycerol, 10 mM Tris base, pH 6.8, 100 mM DTT and 0.01% bromophenol blue) and denatured by heating at 95 °C for 5 min. Samples were then separated on 8% or 10% (depending on the size of the target protein) polyacrylamide gels (running gel composition: 375 mM Tris base, pH 8.8, 10% or 15% acrylamide/bis solution (29:1), 0.1% SDS, 0.1% ammonium persulfate (APS), 0.03% TEMED; stacking gel composition: 125 mM Tris base, pH 6.8, 5% acrylamide/bis solution (29:1), 0.1% SDS, 0.1% APS, 0.08% TEMED) by gel electrophoresis. Electrophoresis was carried out first at 80 V for 10 min and then at 150 V as long as needed in electrophoresis buffer (25 mM Tris base, 192 mM glycine, 0.1% SDS) using the Mini Protean 3 electrophoresis system (Biorad[®]). The Precision Plus Protein Standard[™] was used as molecular weight marker. After separation proteins were transferred onto a nitrocellulose membrane at 300 mA for 90 min in transfer buffer (50 mM Tris base, 380 mM glycine, 0.1% SDS, 20% methanol) using the Mini Trans-Blot cell system. Then the membrane was stained with Ponceau S to

visualize the transferred proteins. After 3 times washing with TBS-T buffer (100 mM Tris base, pH 7.5, 150 mM NaCl, 0.1% Tween 20), the membrane was blocked in milk solution (2.5% BSA, 5% milk powder in TBS-T buffer) for 1 h at room temperature and then, after repeated washing, incubated with the primary antibody (Table 2.1) overnight at 4 °C. After 3 times washing with TBS-T buffer, the membrane was then incubated with the secondary antibody (Table 2.1) for 1 h at room temperature. After two times washing with TBS-T buffer and two times with TBS (100 mM Tris base, pH 7.5, 150 mM NaCl) the membrane was incubated with a detection reagent according to the instruction manual of the SuperSignal[®] West Dura extended duration substrate. The produced chemiluminescent signal was detected with the Chemie Genius² Bio Imaging System and quantified with the Gene Tools[®] software.

Protein	Primary antibody	Dilution	Secondary antibody	Dilution
cMyBP-C	cMyBP-C	1:2000	anti-rabbit IgG peroxidase conjugate	1:7500
Mono- and Poly-ubiquitinated proteins	Ubiquitin	1:50 000	anti-mouse IgG peroxidase conjugate	1:20000
pACC	pACC	1:10000	anti-rabbit IgG peroxidase conjugate	1:10000
β 5-subunit of the 20S proteasome	β 5	1:10000	anti-rabbit IgG peroxidase conjugate	1:10000
Calsequestrin	CSQ	1:10000	anti-rabbit IgG peroxidase conjugate	1:10000

Table 2.1: Antibodies used for protein analysis in tissue.

In the beginning we used the monoclonal anti-ubiquitin antibody from SantaCruz[®] (P4D1). This antibody did not show the typical smear at high molecular weights (data not shown). Moreover there were some unexpected bands showing an untypical pattern. Due to binding problems we switched to the FK2 antibody from Biomol[®]. The SantaCruz[®] was raised against all 76 amino acids of ubiquitin. In contrast the antibody of Biomol[®] binds to Lysin²⁹ Lysin⁴⁸ and Lysin⁶³- linked to mono- und polyubiquitinated proteins, but not to free ubiquitin. This could explain the different patterns obtained with either antibody.

2.2.3 Chymotrypsin-like activity of the proteasome

As described in the introduction, the 20S proteasome contains 3 peptidase activities: the chymotrypsin-like, the trypsin-like and the caspase-like activities. All 3 activities can be determined by measurement of fluorescence generated from enzymatic cleavage of fluorogenic substrate. For the chymotrypsin-like activities, the substrate is Succinyl-leucyl-leucyl-valyl-tyrosyl-7-amino-4-methylcoumarin (SUC-Leu-Leu-Val-Tyr-AMC) (Fig. 2.3).

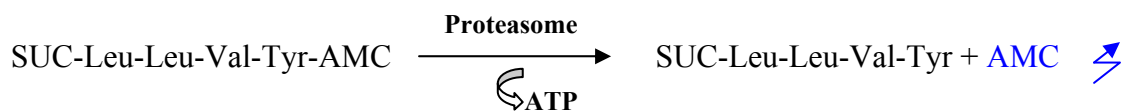


Figure 2.3: Enzymatic reaction during degradation by the 20S proteasome.

To measure the chymo- trypsin-like activity of the 20S proteasome, a specific fluorogenic substrate was used, which was composed of a chain of amino acids and a fluorescent reporter (AMC). After cleavage of this substrates by the chymotrypsin-like activity, the fluorescent reporter is released, whose fluorescence can be measured.

The method to measure the 20S proteasome activity was adapted from (Ludwig et al., 2005). For determination, 30 µg of protein (2.1.1.1) were incubated in the dark for 1 h at 37 °C in an incubation buffer (225 mM Tris-HCl, pH 8.2, 45 mM KCl, 7.5 mM Mg(CH₃COO)₂-4H₂O, 7.5 mM MgCl₂-6H₂O, 1.1 mM DTT) containing an ATP regenerating system (6 mM ATP, 5 mM phosphocreatine, 0.2 U phosphocreatine- kinase) and 60 µM of specific fluorogenic substrate (Figure 2.3).

Released fluorescence of the fluorescent reporter 7-amino-4-methylcoumarin (AMC) was measured using the TECAN[®] Safire[®] microplate reader using two different excitation wavelengths (380 and 350 nm), and two different emission wavelengths of (460 and 450 nm). Each sample was measured in triplicate. The mean of the blank (incubation buffer and H₂O) was subtracted from the mean of each sample triplicate.

In preliminary experiments performed by Saskia Schlossarek, the substrate-dependent and protein amount-dependent response of this method was tested for the chymotrypsin-like activity. To investigate the substrate-dependent response, 10 µg of protein were incubated in incubation buffer with different concentrations of the fluorogenic substrate, whereas different amounts of protein were incubated in incubation buffer containing 60 µM fluorogenic substrate to examine the protein-dependent response of activity (Fig. 2.4).

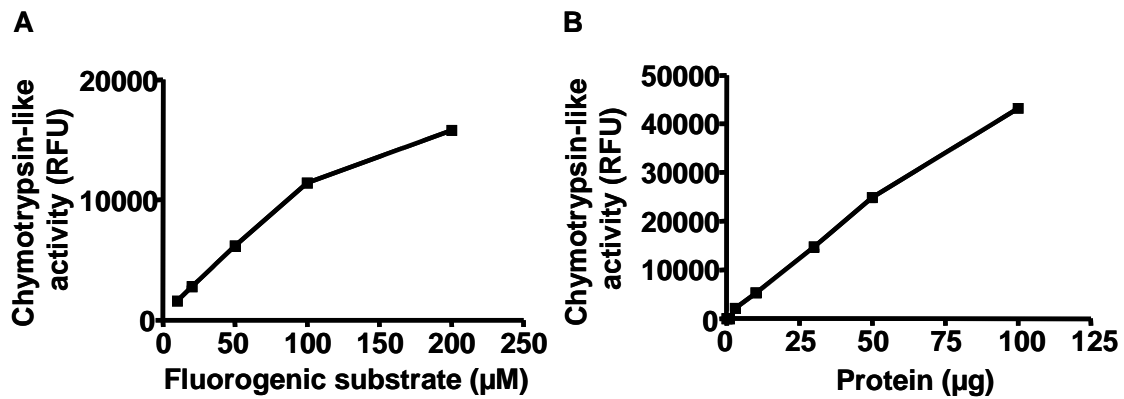


Figure 2.4: Substrate- and protein-dependent response of the chymotrypsin-like activity.

A, Ten µg of protein were incubated for 1 h in incubation buffers with different concentrations of the fluorogenic substrate (SUC-Leu-Leu-Val-Tyr-AMC). **B**, Different amounts of protein were incubated for 1 h in incubation buffer containing 60 µM fluorogenic substrate (SUC-Leu-Leu-Val-Tyr-AMC). For A and B, released fluorescence was measured at an excitation wavelength of 380 nm and an emission wavelength of 460 nm. Experiment performed by Saskia Schlossarek.

In both experiments, an almost linear increase of the fluorescence intensity was observed. With regard to the substrate-dependent response, it seems that the system starts to be saturated when high concentrations of fluorogenic substrate (200 µM) were used.

2.2.4 Immunoprecipitation and tandem mass spectrometry

To find specific ubiquitinated candidates, immunoprecipitations with subsequent tandem mass spectrometry were performed in collaboration with Dr. Buck (Institute of Cell Biology and Clinical Neurobiology, University Hospital Eppendorf Hamburg, Germany). Proteins were extracted in the same way as mentioned before but with RIPA high salt buffer to lyse cytoplasmic, membrane and nuclear proteins. 2 g of ventricular proteins of 10 week- (wk) old animals were filled up to 10 ml with RIPA high salt buffer. Fifty µg of the FK2 antibody of Biomol[®] were added. To capture the immune complexes 600 µl of Protein G beads conjugated with sepharose from SantaCruz[®] were used. After the beads were washed by centrifugation they were resuspended in Lämmli buffer and boiled at 95°C for 5 min to dissociate the proteins before loading them on a polyacrylamid gel.

The visible bands were cut out and given to the laboratory of Dr. Buck, who analyzed the bands. The proteins were cut into peptides by Trypsin to conduct them to a MALDI-TOF tandem mass spectrometry for peptide sequencing. The detected peptides were compared

with Mascot[®] data base for peptide finger printing.

2.2.5 Statistical analysis

Data are presented as mean±SEM. Statistical analyses were performed using the unpaired Student's t-test. Spearman correlation and linear regression analyses were performed to assess the relationship between hypertrophy, ubiquitination and degradation in the homozygous cMyBP-C KO mice. Analyses were performed using commercial software (GraphPad[®] Software, Inc.). A value of $P < 0.05$ was considered statistically significant.

3 Results

3.1 Determination of the degree of cardiac hypertrophy

We first investigated the cardiac phenotype in cMyBP-C-KO and WT mice by determining the HW/BW ratio over 7 postnatal time points.

3.1.1 Investigation of KO mouse phenotype: heart weight and body weight ratio

Both mouse lines increased their body BW with similarly shaped curves. After 9 wks of age the growth slowed down, but still augmented to a final weight at 50 wks of 36.4 g in the KO mice and of 32.2 g in WT mice (Figure 3.1A). The HW increased as expected in both mouse lines. However, the KO mouse line had a greater growth over all ages, except at 2 wks, where there was a tendency but no significance. The HW was 67% higher at 50 wks of age in KO than in WT mice (Figure 3.1B).

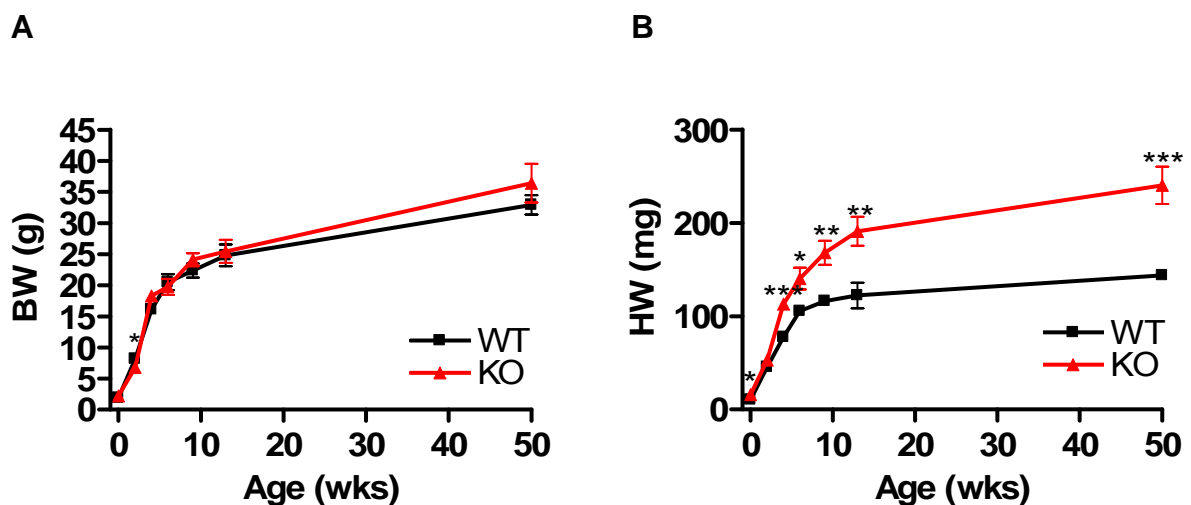


Figure 3.1: Body and heart weights of WT and KO mice.

A shows the increase in the body weight (BW). B shows the heart weight (HW) over all ages except at 2 wks. Points represent the mean \pm SEM *P<0.05, **P<0.01 *** P<0.001 vs. WT, Student's t- test. The number of animals was n=6, except in KO 50 wks it was n=5.

3.1.2 Investigation of the mouse cardiac phenotype

HW/BW ratio was calculated for each animal to exclude a bias because of different animal

weights. The WT mice exhibited a decrease in the HW/BW ratio over age (NN vs. 50 wks $p < 0.05$ student's t-test). In contrast, KO mice did not show major differences over times (Figure 3.2). During all post-natal development, the HW/BW ratio was higher in KO compared to WT mice. At 13 wks of age, the HW/BW ratio was 55% higher in the KO group. The percentage of change in HW/BW ratio in KO compared to WT is shown in Figure 3.2B and in table 3.1. In Figure 3.2C are shown 43 wk-old WT and apple-shaped hypertrophied KO hearts. Taken the mean of all animals overtime, KO mice exhibited 36% higher HW/BW compared to WT mice (Figure 3.2D).

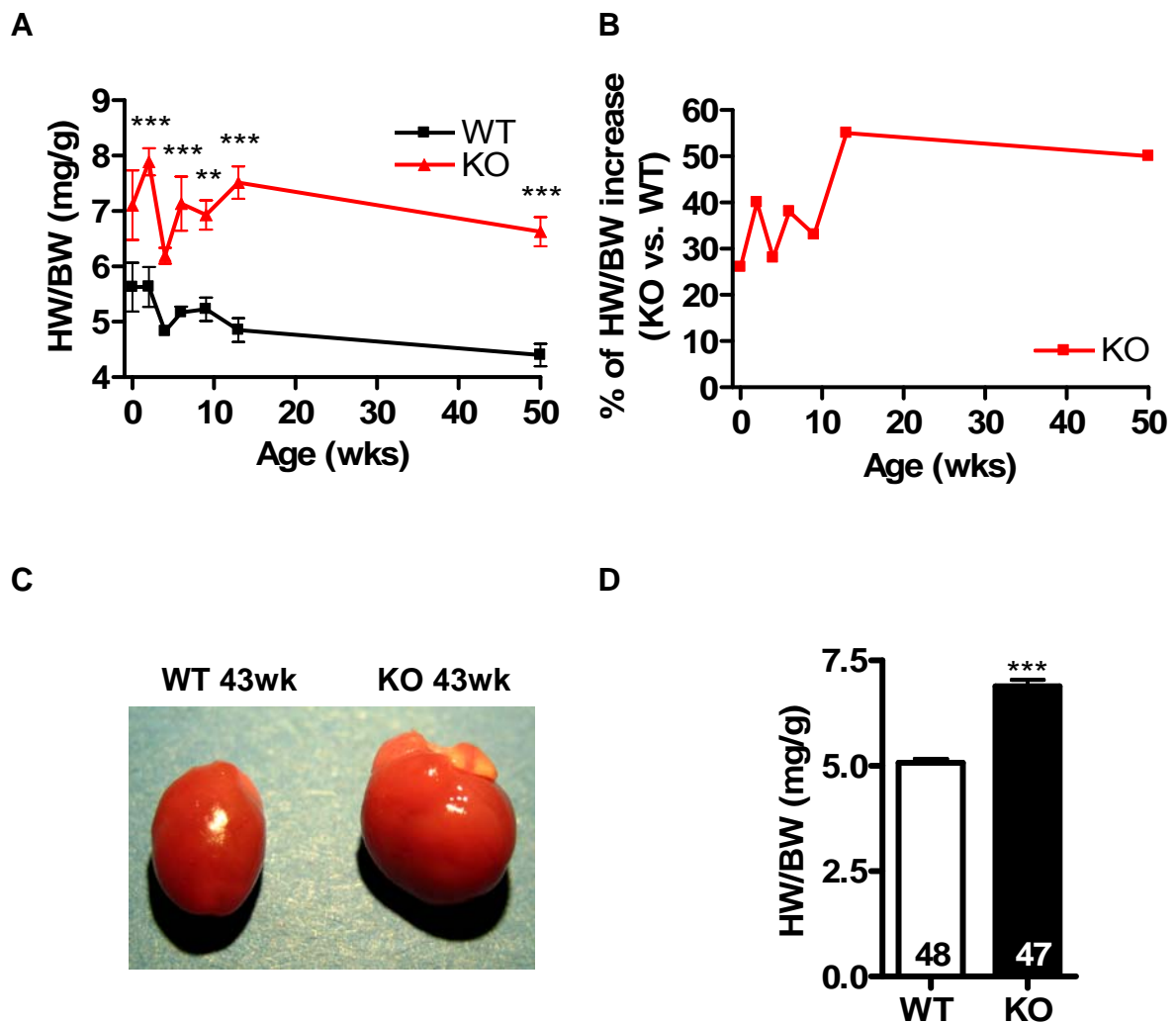


Figure 3.2: Heart weight to body weight ratio in WT and KO.

Mice and extracted hearts were weighed. **A**, The heart weight to body weight ratio (HW/BW) was determined at 7 different post-natal time points in KO and in corresponding WT mice. **B**, Percentage of increase of HW/BW in KO relative to WT over time. **C**, Representative hearts of 43 wk-old male WT and KO mice. **D**, Mean values of HW/BW ratio from all the KO and WT mice. Bars represent the mean \pm SEM, ** $P < 0.01$ and *** $P < 0.001$ vs. WT, Student's t- test. The number of animals was $n=6$ except in KO 50 wks it was $n=5$. The number of animals is indicated in the bars.

Age (wks)	NN	2	4	6	9	13	50
Change	+26%	+40%	+28%	+38%	+33%	+55%	+50%
P value	0.08	<0.001	<0.001	<0.01	<0.001	<0.001	<0.001

Table 3.1: Percentage of change of the HW/BW ratio in KO relative to WT.

The results of Figure 3.2B are shown tabularly. Student's t-test. The number of animals was n=6 except in KO 50 wks it was n=5.

3.1.3 Summary

The major findings of this part were the following:

- The KO mice exhibited an apple-shaped hypertrophied heart and a higher HW, but no lower BW compared to WT.
- Shortly after birth KO mice showed higher HW/BW ratio already.
- The mean HW/BW ratio over time was 36% higher in KO mice than in WT mice.

3.2 Determination of calsequestrin amount in KO and WT mice

In order to compare the amount of protein from one blot to another, we needed to normalize the level of protein of interest to an endogenous protein that should not vary between KO and WT mice. We investigated whether calsequestrin (CSQ) levels changes with post-natal development. For this experiment the ventricular proteins of 8 gender-matched animals were pooled at each age. We used an antibody directed against CSQ and performed Western blot analysis. Figure 3.3A shows a representative Western blot of CSQ. The data shown in Figure 3.3B summarizes data obtained from several CSQ blots. The variations between the mouse lines are due to slight loading differences. Both mouse lines showed increase in CSQ expression over age. These data indicate that CSQ cannot be used to compare the different time points, but can be used at each time point.

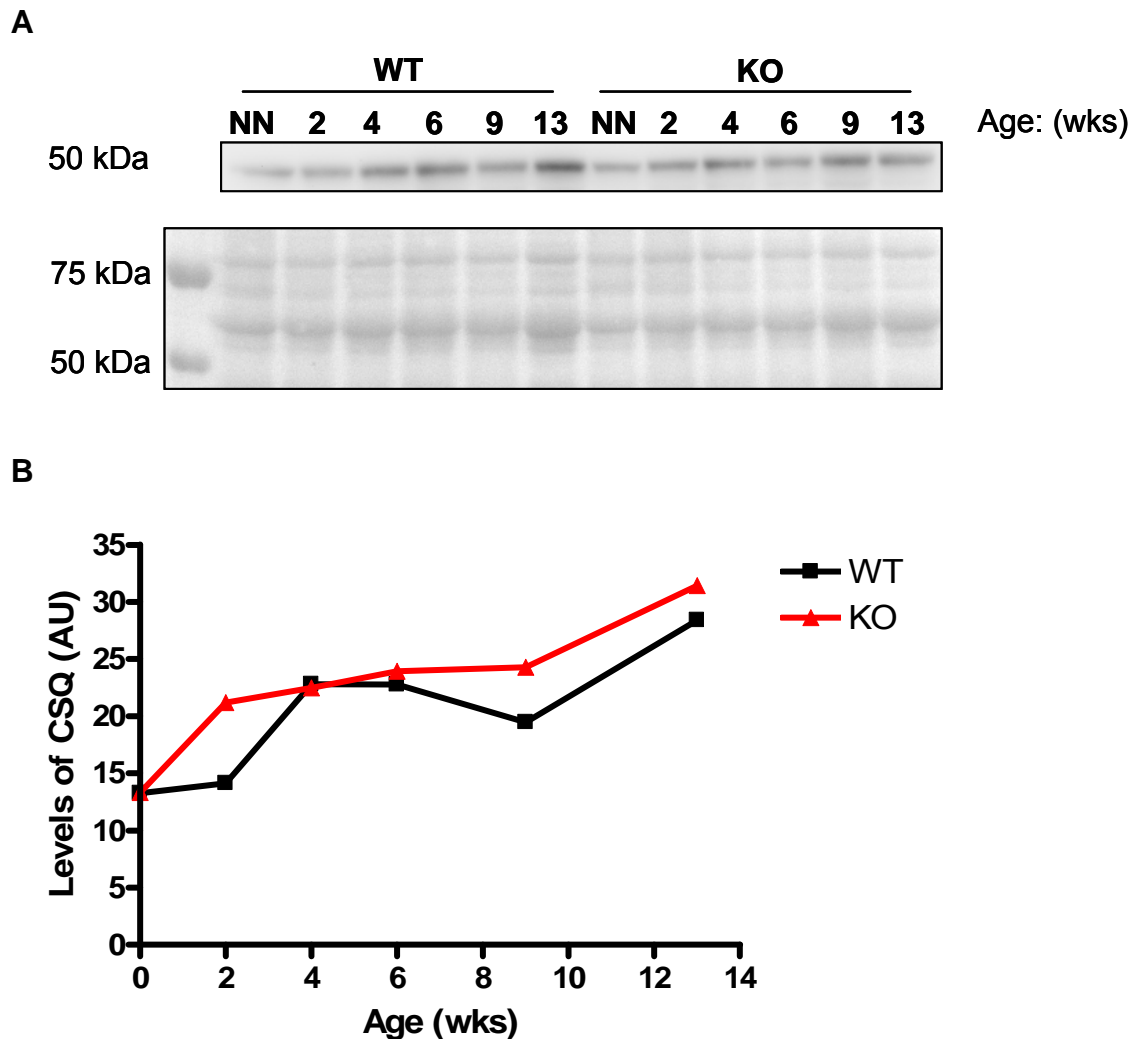


Figure 3.3: Evaluation of the profile of the level of CSQ during post-natal development.

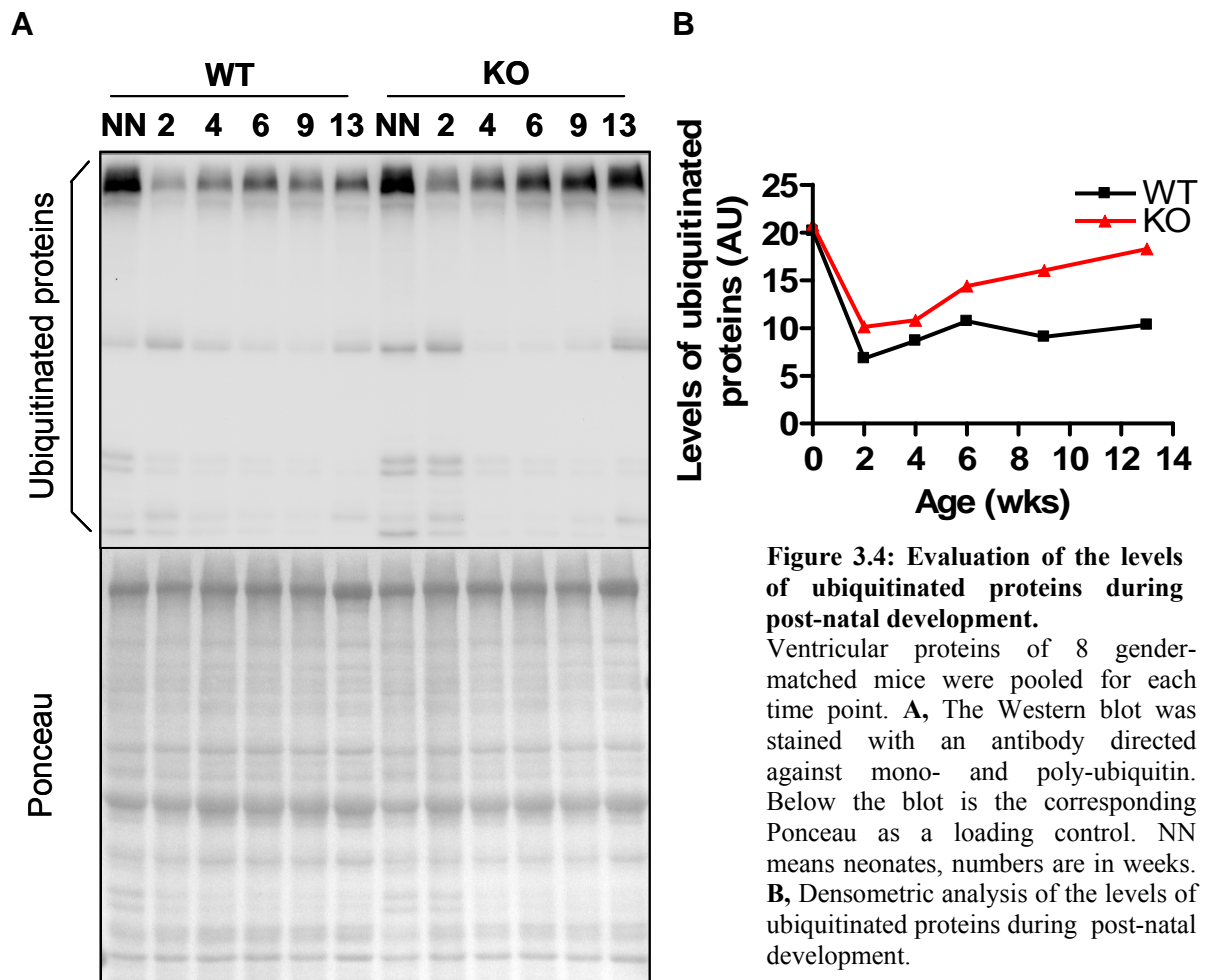
The ventricular proteins of 8 gender-matched animals were pooled for each time point. **A**, The representative blot was stained with an antibody directed against CSQ. Below the blot is the corresponding Ponceau. NN means neonates; numbers are in weeks. **B**, Densitometric analysis of the different time points during post-natal development (raw data).

3.3 Determination of the steady-state levels of ubiquitinated proteins

We hypothesized that the UPS might be involved during the evolution of hypertrophy. We therefore investigated the steady-state levels of ubiquitinated proteins by Western blot analysis. The antibody was the FK2 against mono- and poly-ubiquitin forms from Biomol[®]. As expected, it binds to several ubiquitinated proteins producing the typical smear at high molecular weights (Figure 3.4).

3.3.1 Investigation of ubiquitinated proteins over age

We first pooled the ventricular protein extracts from 8 gender-matched mice to have an overview of the levels of ubiquitinated proteins overtime on one blot, as shown before for CSQ.



The steady-state level of ubiquitinated-proteins was elevated at birth, dropped quickly thereafter and remained low with post-natal development in WT mice. Similarly, in KO mice the amount of ubiquitinated proteins was also high at birth and dropped in the first 2 wks of age. Furthermore, KO hearts exhibited a higher amount of ubiquitinated proteins after 6 wks of age compared to WT mice (Figure 3.4).

3.3.2 Steady-state levels of ubiquitinated proteins at different post-natal time points

We then precisely quantified the steady-state levels of ubiquitinated proteins in KO and WT mice at each postnatal time point. Ventricular extracts were analyzed for NN, 2 wk-, 4 wk-, 6 wk-, 9 wk-, 13 wk- and 50 wk-old mice (Figure 3.5). No major difference in the steady-state level of ubiquitinated proteins was observed between KO and WT neonatal mice. Similar results were obtained at 2 and 4 wks of age (data not shown). At 6 wks of age KO mice exhibited 122% higher steady-state levels of ubiquitinated proteins than WT mice (Figure 3.5A, B). Then the levels remained between +36% and +54% higher in KO than in WT mice. These results fit to the data obtained with the pool of proteins at different post-natal time points (Figure 3.4B).

3.3.3 Investigation of specific ubiquitinated candidates

In the different Western blots shown in Figure 3.5, a band of about 60 kDa seemed to be more abundant in KO than in WT mice. We hypothesized that it could be a specific ubiquitinated protein candidate, which could lead to or result from alterations of the UPS in the KO mice (Figure 3.4). In order to isolate a specific ubiquitinated candidate we performed immunoprecipitations with subsequent tandem mass spectrometry (MS/MS), which were done by Dr. Buck. For these experiments we used the same FK2 antibody from Biomol® as for the Western blot analysis. After staining a polyacrylamid gel with Coomassie the visible bands were cut out, the proteins extracted out of the gel portion and conducted to tandem mass spectrometry. Peptides were identified by Peptide Mass Finger Printing. The cardiac protein samples used were from 10 wk-old animals. In a last experiment we compared the results of immunoprecipitation of KO and WT on the same blot.

The only protein of interest we detected by mass spectrometry was desmin (53-55 kDa) which is known to be ubiquitinated (Taylor et al., 1995). The amino acid sequence found with the MS/MS was FLEQQNAALAAEVNR (Figure 3.4D). The Mascot Matrix® found: Q9JJY2_MOUSE, Desmin (Fragment).- Mus musculus (Mouse). Moreover, ubiquitin was detected in the same band (data not shown), suggesting that desmin was ubiquitinated, because the FK2 antibody pulls down only ubiquitinated proteins. In the other bands ubiquitin and a lot of not attributable peptides were found (Figure 3.5C).

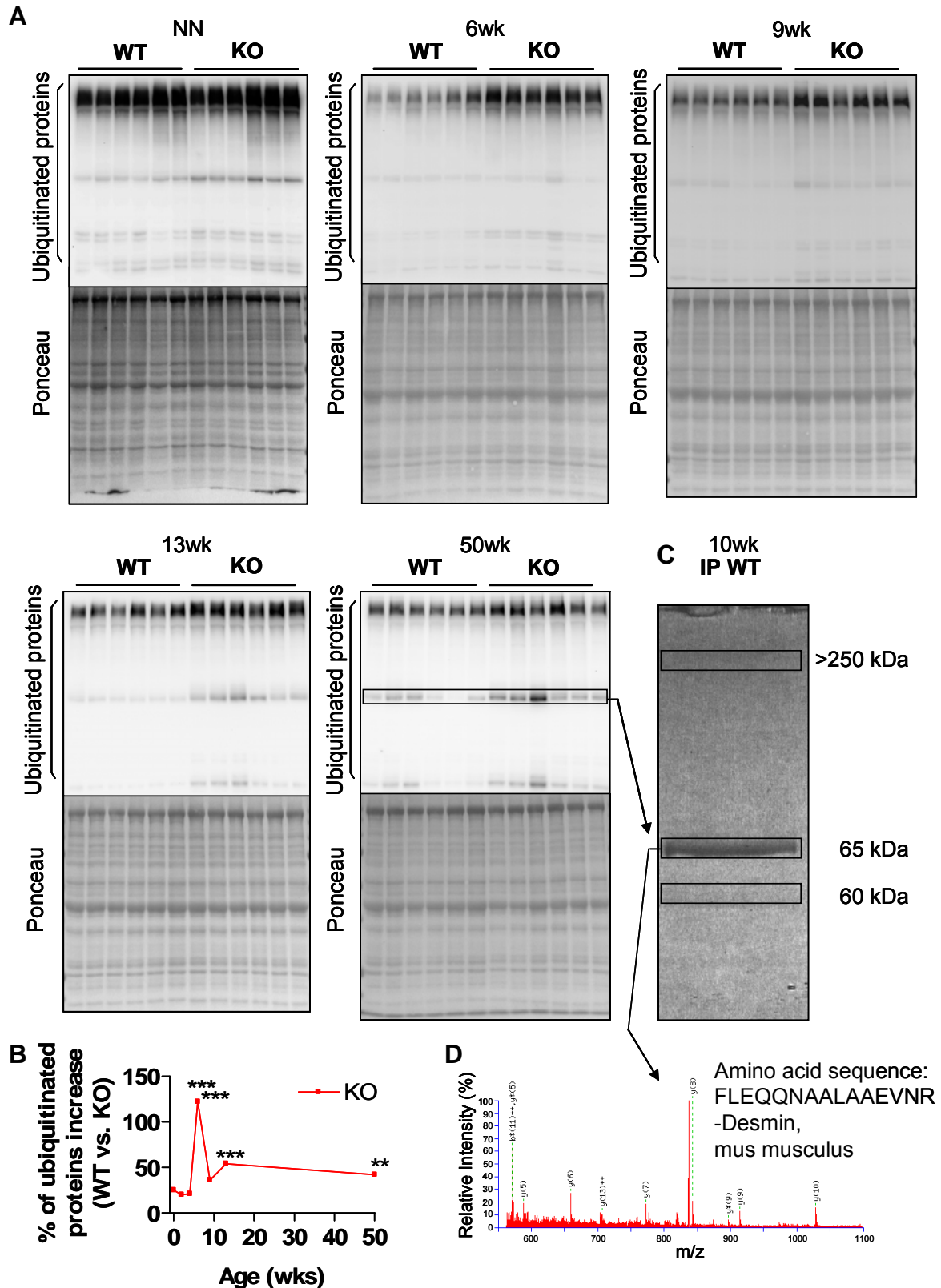


Figure 3.5: Steady-state levels of ubiquitinated proteins in KO vs. WT at different post-natal ages. Ventricular proteins of 6 gender-matched animals of each mouse line were extracted for each time point. **A**, The Western blots (2 and 4wks not shown) were stained with an antibody directed against ubiquitin. Below the blot is the corresponding Ponceau as loading control. **B**, Percentage of increase in KO vs. WT mice. $^{**}P < 0.001$, $^{***}P < 0.001$, Student's *t*-test, number of animals was $n = 6$, except in KO 50 wks ($n = 5$). NN means neonates. **C**, Investigation of specific ubiquitinated candidate. An immunoprecipitation of ventricular protein of a 10 wk-old WT mouse with an antibody directed against mono- and poly-ubiquitinated proteins was performed. Coomassie stained gel is shown with the cut band, which were dissolved for subsequent tandem mass spectrometry. **D**, Mass spectrum with peak corresponding to a peptide of desmin. The amino acid sequence is shown beside the peak.

In Western blot analysis particularly in NN, 13 wk- and 50 wk-old animals' bands around 60 kDa with higher levels of ubiquitinated proteins were noticeable in KO compared to WT mice. To investigate whether it is specific in the KO, we performed an immunoprecipitation from both KO and WT ventricular proteins in parallel. The immunoprecipitates were loaded on a gel subsequently stained with Coomassie. Unexpectedly there was no additional band in the KO and both mouse lines showed in their appearance five identical of bands. The following MS/MS did not reveal any specific proteins and any difference between the two mouse lines (Figure 3.6).

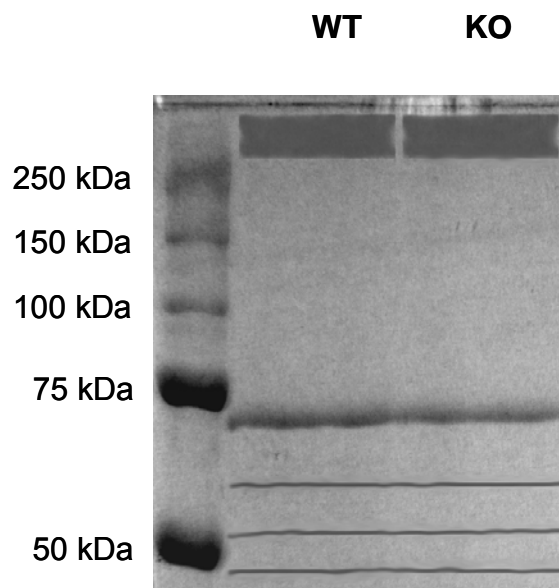


Figure 3.6: Comparison of band patterns after immunoprecipitation in WT and KO samples. Immunoprecipitations of a 10 wk-old WT and KO mice with an antibody directed against mono- and poly-ubiquitinated proteins. The polyacrylamid gel was stained with Coomassie blue (bands digitally enhanced).

3.3.4 Summary

The major findings of this part were the following:

- The steady-state levels of ubiquitinated proteins were very high at birth and dropped shortly thereafter in both KO and WT mice.
- The KO showed higher levels of ubiquitinated proteins from 6 wks on suggesting that there are alterations of the UPS in mice lacking cMyBP-C.
- No specific candidate protein with higher ubiquitination was found in KO mice.

3.4 Investigation of protein degradation

3.4.1 Determination of the chymotrypsin-like activity in KO and WT mice

To investigate whether the higher steady-state levels of ubiquitinated proteins result from proteasome impairment in the KO hearts, chymotrypsin-like activity of the proteasome, which is the main proteasome activity, was determined in ventricular cytosolic extracts from both KO and WT mice. This was performed by Saskia Schlossarek.

At birth, there was no difference in the chymotrypsin-like activity between the two mouse lines (Figure 3.7). Then, at 2 wks of age a 27% greater activity was found in KO than in WT. At the age of 6 wks a >50% greater activity was measured which remained higher in the KO mice up to the age of 50 wks. The trypsin-like activity and caspase-like activity were also higher in the KO compared to WT (data not shown).

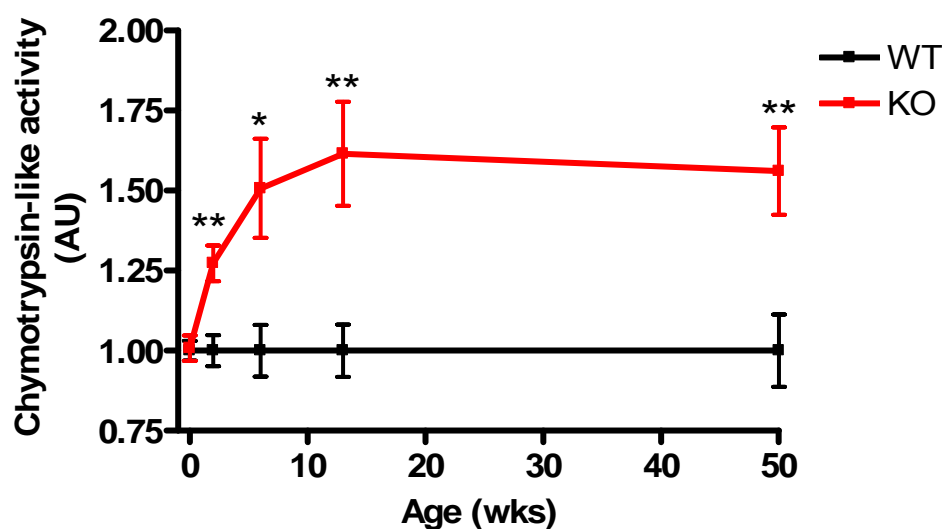


Figure 3.7: Chymotrypsin-like activity of the proteasome in the KO and WT hearts.

Ventricular cytosolic proteins were extracted from gender-matched KO and WT littermates. The time course shows the quantitative analysis of samples in neonates, 2 wk-, 6 wk-, 13 wk- and 50 wks-old animals. Symbols represent the mean \pm SEM. *P<0.05, **P<0.01, vs. WT. Student's t- test. The number of animals for each time point was n=8 in both mouse lines.

3.4.2 Determination of the levels of the β 5-subunit of the 20S proteasome

To determine whether the higher chymotrypsin-like activity in the KO results from a higher amount of the protein carrying this protease activity, we determined the level of the β 5-subunit of the 20S proteasome by Western blot analysis using a specific antibody

(kindly given by X. Wang, Sioux Fall, SD).

We first evaluated the expression pattern of the $\beta 5$ -subunit during post-natal development using the pool of proteins. The level of $\beta 5$ -subunit dropped shortly after birth in the WT mice (Figure 3.8). At 4 wks of age the amount was 34% of the initial level and remained low during all the postnatal development (Figure 3.8). Similar to WT, the amount of $\beta 5$ -subunit dropped continuously in KO mice. The level of $\beta 5$ did not differ between KO and WT, except at 2 wks of age, where it was higher in KO.

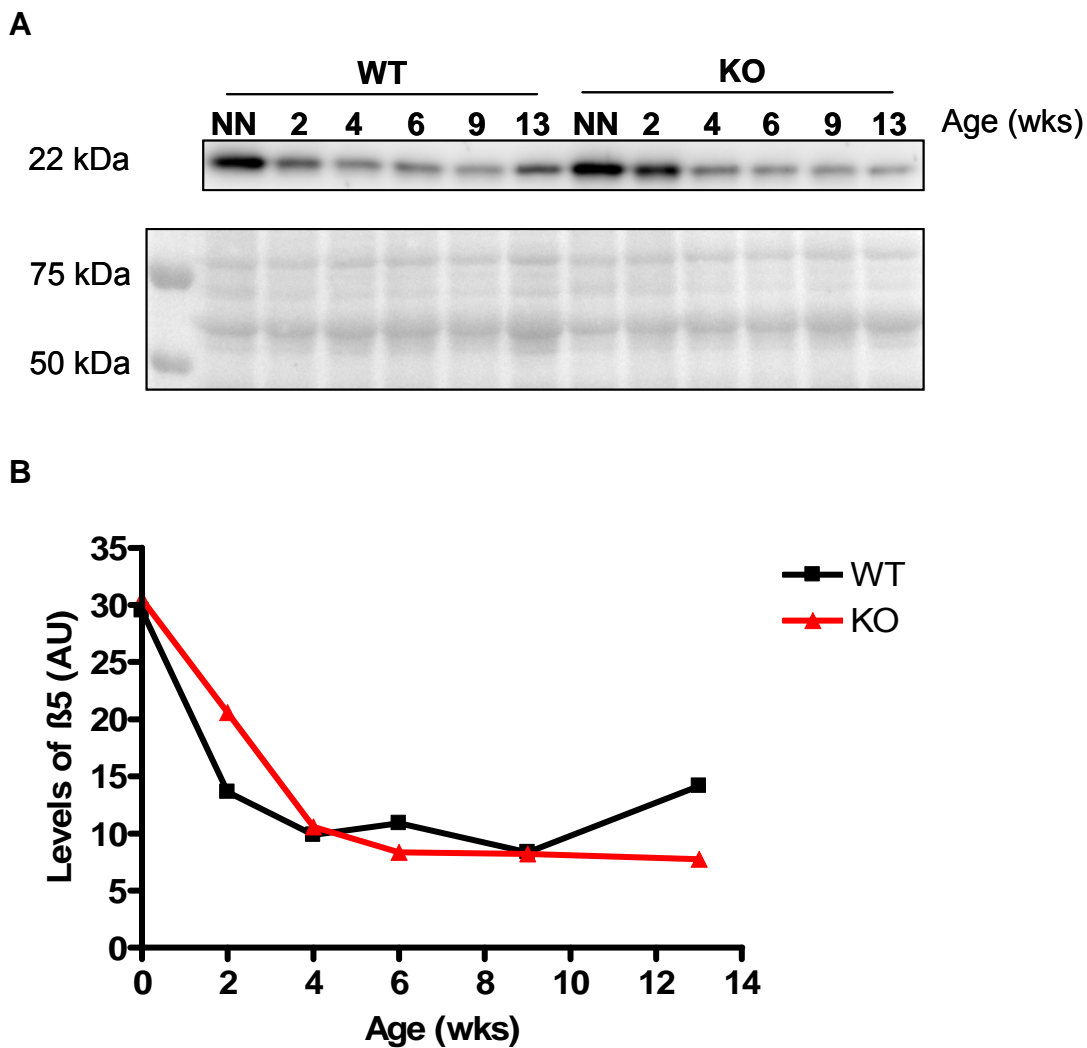


Figure 3.8: Evaluation of the profile of expression of the $\beta 5$ -subunit of the proteasome during post-natal development.

Cytosolic ventricular proteins of 8 gender-matched animals were pooled for each time point. **A**, The Western blot was stained with an antibody directed against $\beta 5$. Below the blot is the corresponding Ponceau as loading control. NN means neonates, numbers are in weeks. **B**, Quantitative analysis performed at different time points.

In order to precisely quantify and compare the level of $\beta 5$ -subunit in KO and WT mice, we evaluated its level and normalized it to CSQ at seven post-natal time points. A representative Western blot of the neonates is shown in Figure 3.9A. The level of $\beta 5$ -subunit did not differ in WT and KO mice, except at birth where it was 24% lower in KO (Figure 3.9B). We therefore pooled all the samples and found similar levels of $\beta 5$ -subunit in KO and WT ventricles (Figure 3.9C). This suggests that the higher chymotrypsin-like activity of the proteasome does not result from a higher amount of $\beta 5$ -subunit in KO compared to WT mice.

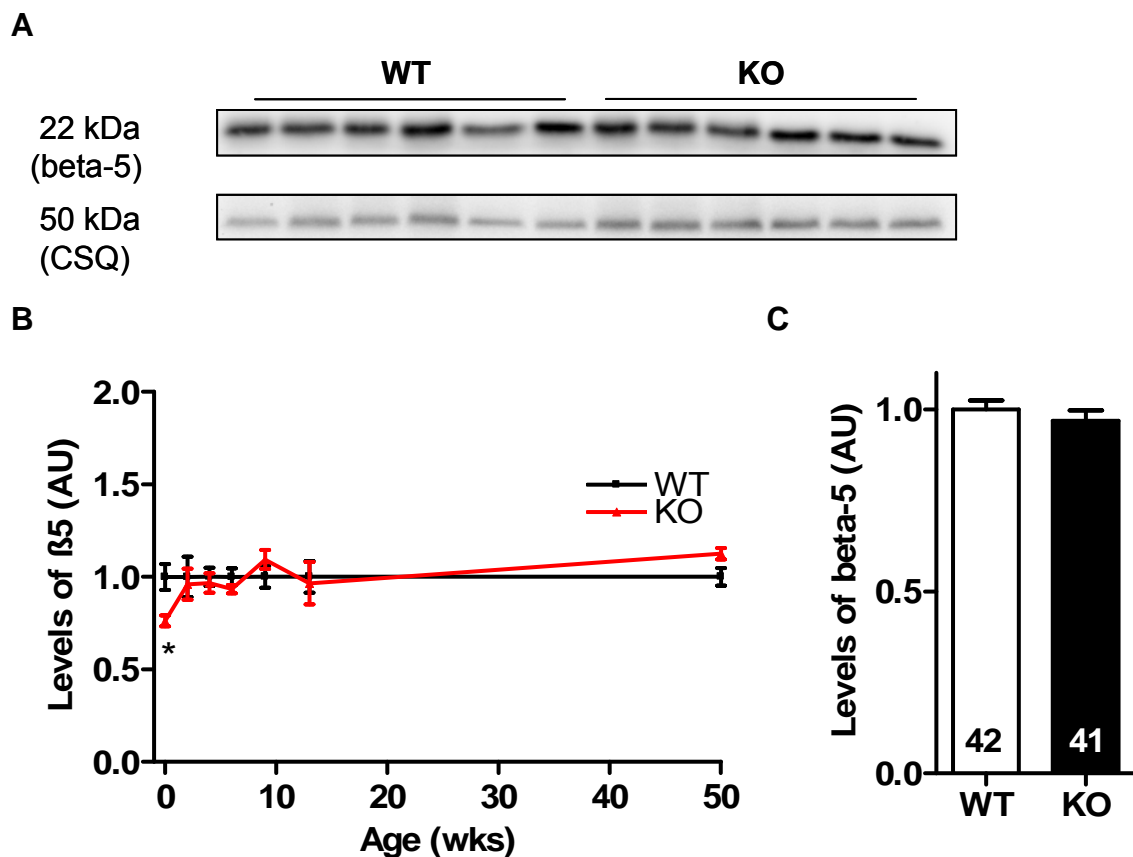


Figure 3.9: Investigation of the $\beta 5$ -subunit levels in KO and WT mice.

Ventricular proteins from gender-matched animals of seven different time points of KO and WT mice were extracted. **A**, The Western blot was stained with an antibody directed against the $\beta 5$ -subunit. The 6 wk time point is shown. Below the blot is the corresponding CSQ Western blot as loading control. **B**, Quantitative analysis performed at different time points. Mean \pm SEM values of $\beta 5$ from all the KO and WT mice. * $P < 0.05$, vs. WT. Student's t-test. The number of animals was $n = 6$, except in KO 50 wks it was $n = 5$. **C**, Bars represent the mean \pm SEM. Number of animals is indicated in the bars.

3.4.3 Investigation of ATP-depletion

Since the UPS is an ATP-dependent system, we hypothesized that the higher chymotrypsin-like activity could result in ATP depletion in KO hearts. The ATP depletion was measured indirectly by determining the amount of phosphorylated acetyl-CoA carboxylase (pACC), a 250 kDa protein, which is a product of the AMP-kinase (Figure 3.10). The activity of the AMP-kinase is inversely correlated to the ATP-level (Hardie et al., 1999). Interestingly, as for the steady-state levels of ubiquitinated proteins, the level of pACC was high at birth and immediately dropped after (Figure 3.11).

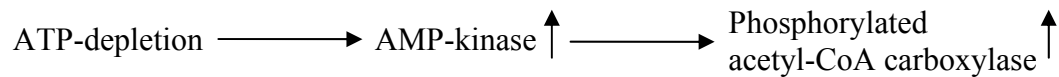


Figure 3.10: Enzymatic reaction following ATP-depletion.

To measure the ATP-depletion of ventricular cells we determined the level of phosphorylated acetyl-CoA carboxylase, which is phosphorylated by the AMP-kinase when ATP is depleted.

At 2 wks of age, the pACC level was 10% of the NN level. Then the levels of pACC slightly augmented in both WT and KO mice. Interestingly, the level of pACC was similar in both KO and WT at all post-natal time points.

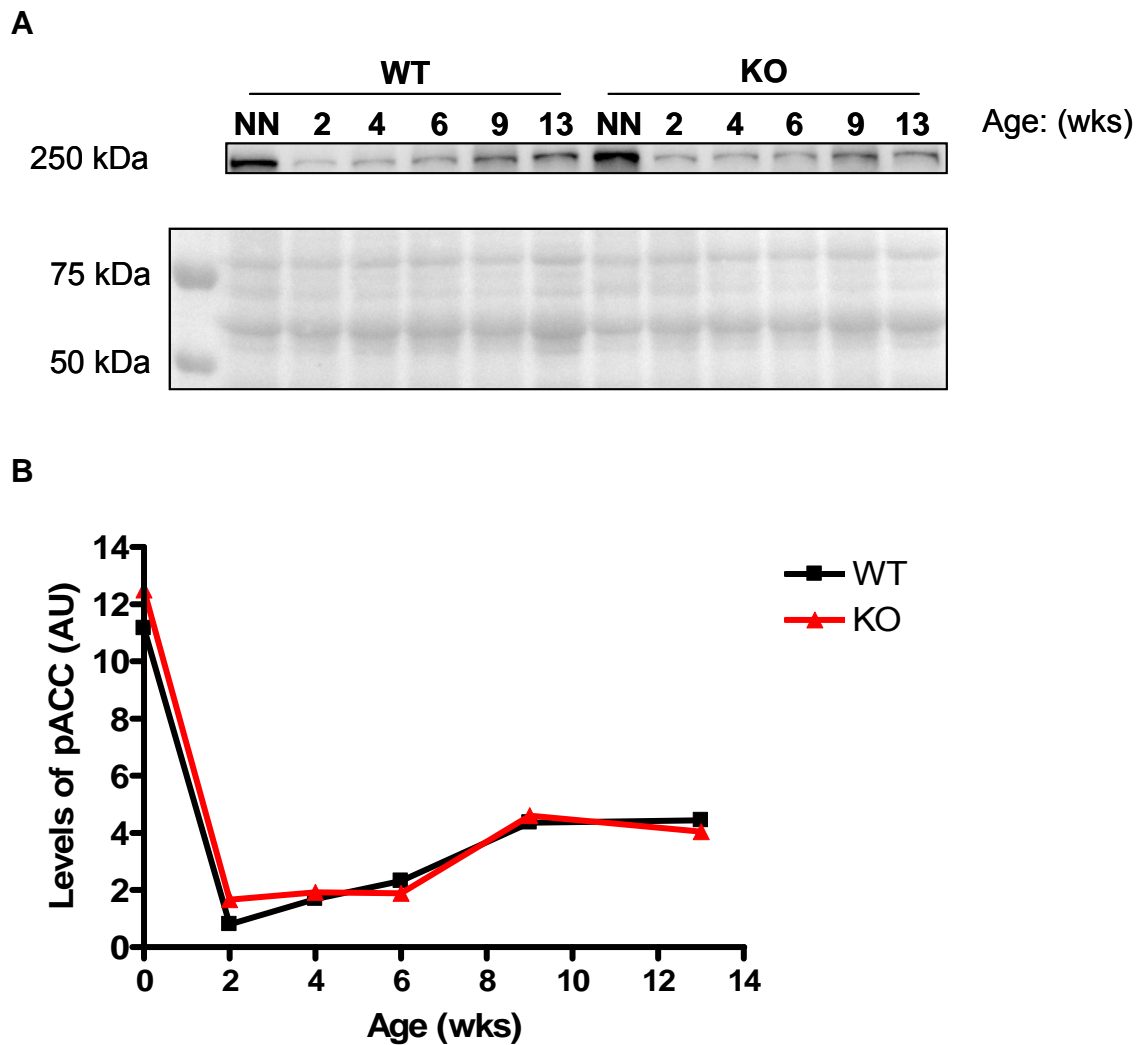


Figure 3.11: Evaluation of the profile of expression of pACC during post-natal development.

The ventricular proteins of 8 gender matched animals were pooled for each time point. **A**, The blot was stained with an antibody directed against phosphorylated acetyl- CoA carboxylase. Below the blot is the corresponding Ponceau as loading control. NN means neonates, numbers are in weeks. **B**, Quantitative analysis performed at the different time points.

3.4.4 Determination of the levels of pACC

We then precisely quantified the pACC level at each time point and normalized it to CSQ (Figure 3.12). Figure 3.12A shows a representative Western blot of pACC pattern obtained in 6 wk-old WT and KO mice. This shows a lot of inter-individual variations. However, the evaluation at each time point did not show any difference of the amount of pACC in KO and WT mice (Figure 3.12C).

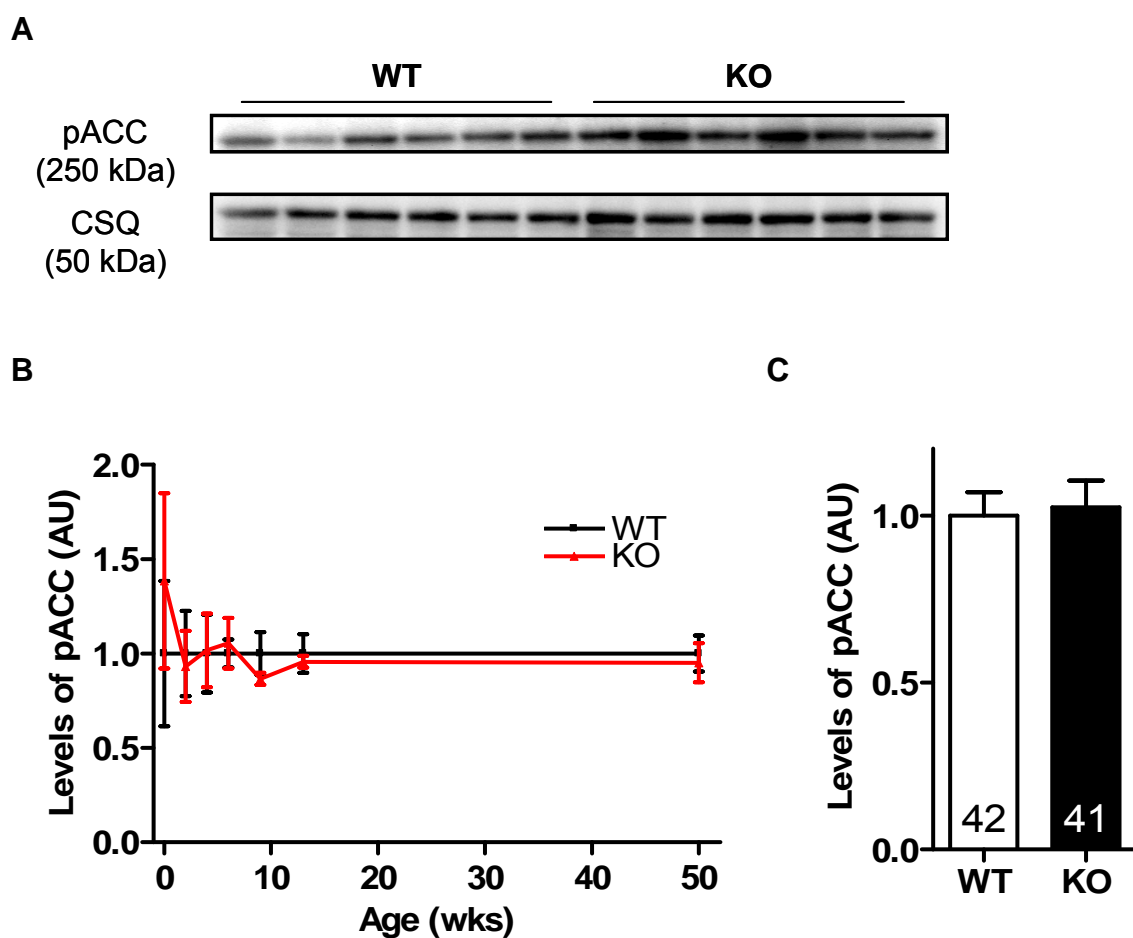


Figure 3.12: Investigation of pACC in KO and WT mice.

Ventricular proteins from gender matched animals of each mouse line were extracted at every time point. **A**, The Western blots were stained with an antibody directed against pACC. The 6 wk time point is shown. Below the blot is the corresponding Calsequestrin as loading control. **B**, Quantitative analysis performed at different time points. Mean \pm SEM values of pACC from all the KO and WT mice. * $P < 0.05$, vs. WT. Student's *t*-test. The number of animals was $n=6$, except in KO 50 wks it was $n=5$. **C**, Bars represent the mean \pm SEM. Number of animals is indicated in the bars.

3.4.5 Summary

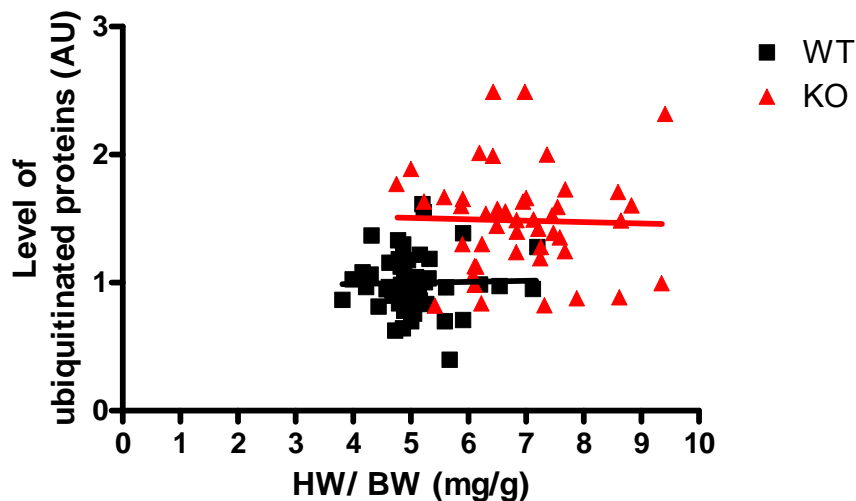
The major findings of this part were the following:

- The chymotrypsin-like activity, which is the main activity of the 20S proteasome, was greater in KO ventricles shortly after birth and remained higher during all post-natal development compared to WT mice.
- The levels of the $\beta 5$ -subunit of the 20S proteasome was very high at birth and dropped shortly after in both groups, without significant differences in KO and WT mice.
- The pACC levels dropped after birth in both groups and did not differ in WT and KO mice.

3.5 Correlations

3.5.1 Correlation between ubiquitination and hypertrophy

We then investigated whether a correlation exists between the degree of UPS alterations and the degree of cardiac hypertrophy. We first evaluated the correlation between the HW/BW ratio and the amount of ubiquitinated proteins (Figure 3.13). Although both parameters were higher in KO than in WT mice, no correlation was found between these parameters in both groups. This suggests that cardiac hypertrophy and high amount of ubiquitinated proteins are independent in KO mice.



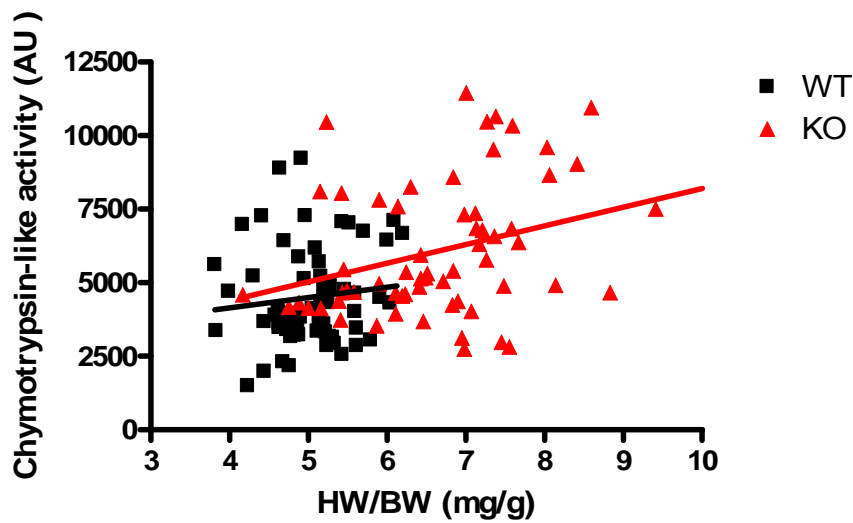
	WT	KO
Spearman r	0.02	-0.03
P value (two-tailed)	0.87	0.84

Figure 3.13: Correlation between the steady-state levels of ubiquitinated proteins and the degree of cardiac hypertrophy in KO and WT mice

The level of ubiquitinated proteins was plotted against the HW/BW ratio. This was analyzed using the non parametric correlation test of Spearman (r). Results are shown below the graph.

3.5.2 Correlation between degradation and hypertrophy

We then evaluated the correlation between the chymotrypsin-like activity and the HW/BW ratio (Figure 3.14). No correlation was found in WT mice. In contrast, a positive correlation ($r=0.39$, $P<0.01$) was found in the KO mice. This suggests that cardiac hypertrophy and high chymotrypsin-like activity are inter-dependent in KO mice.



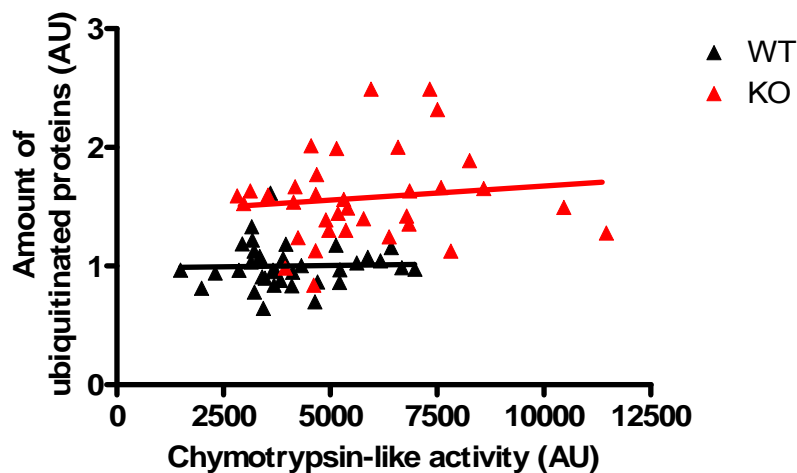
	WT	KO
Spearman r	0.09	0.39
P value (two-tailed)	0.48	<0.01

Figure 3.14: Correlation between the chymotrypsin-like activity and the degree of cardiac hypertrophy in KO and WT mice.

The level of chymotrypsin-like activity was plotted against the HW/BW ratio. This was analyzed using the non parametric correlation test of Spearman (r). Results are shown below the graph.

3.5.3 Correlation between ubiquitination and degradation

We then evaluated the correlation between the chymotrypsin-like activity and the amount of ubiquitinated proteins (Figure 3.15). We expected a negative correlation. Surprisingly, no correlation was found suggesting independence of these parameters in both groups.



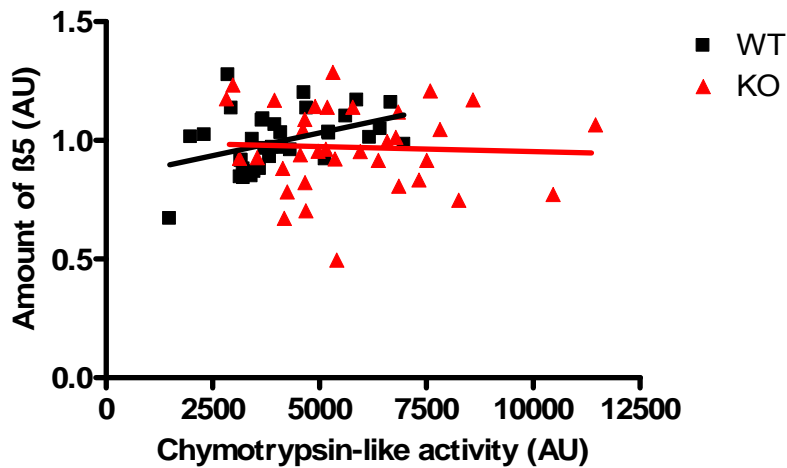
	WT	KO
Spearman r	0.04	0.12
P value (two-tailed)	0.83	0.47

Figure 3.15: Correlation between the steady-state levels of ubiquitinated proteins and the chymotrypsin-like activity KO and WT mice.

The amount of ubiquitinated proteins was plotted against the chymotrypsin-like activity. This was analyzed using the non parametric correlation test of Spearman (r). Results are shown below the graph

3.5.4 Correlation between the amount and activity of the β 5-subunit

We then investigated whether a correlation exists between the amount of β 5-subunit and the chymotrypsin-like activity (Figure 3.16). As expected, a positive correlation between the two parameters was observed in the WT mice (Spearman $r=0.43$, $p<0.01$). In contrast, no correlation between the amount and activity of the β 5-subunit was revealed in the KO mice. This suggests that the higher chymotrypsin-like activity is independent of the level of β 5-subunit in the KO.



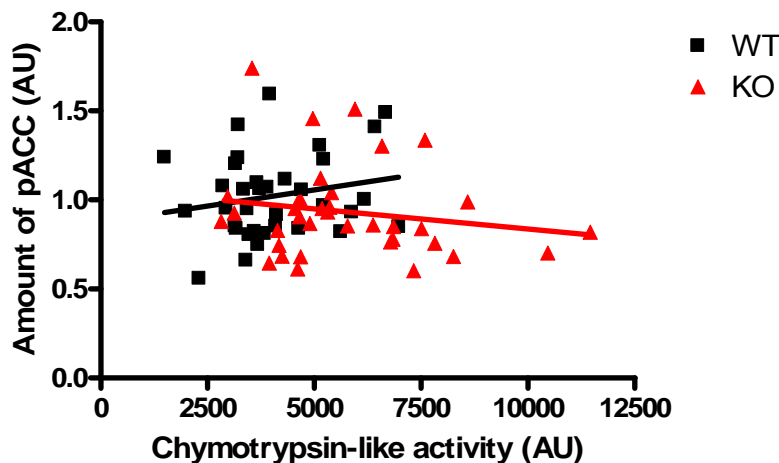
	WT	KO
Spearman r	0.43	-0.06
P value (two-tailed)	0.01	0.74

Figure 3.16: Correlation between the steady-state levels of $\beta 5$ -subunit and chymotrypsin-like activity in KO and WT mice.

The amount of $\beta 5$ was plotted against the chymotrypsin-like activity. This was analyzed using the non parametric correlation test of Spearman (r). Results are shown below the graph.

3.5.5 Correlation between degradation and ATP depletion

We finally evaluated whether a correlation exists between the steady-state levels of pACC (indicator for ATP-depletion) and the chymotrypsin-like activity (Figure 3.17). We expected a negative correlation, i.e., the higher the chymotrypsin-like activity, the lower the amount of ATP and therefore higher the amount of pACC. No significant correlation between the pACC levels and the chymotrypsin-like activity was observed in both groups.



	WT	KO
Spearman r	0.12	-0.13
P value (two-tailed)	0.49	0.47

Figure 3.17: Correlation between ATP-depletion and degradation in KO and WT mice.

The amount of pACC was plotted against the chymotrypsin-like activity. This was analyzed using the non parametric correlation test of Spearman (= r). Results are shown below the graph.

3.5.6 Summary

The major findings of this part were the following:

- The steady-state levels of ubiquitinated proteins did not correlate with the degree of hypertrophy in both groups.
- The chymotrypsin-like activity was positively correlated with the degree of hypertrophy in KO, but not in WT mice.
- Interestingly, no correlation was found between the chymotrypsin-like activity and the levels of ubiquitinated proteins, suggesting that these two parameters vary independently from each other
- The chymotrypsin-like activity was not correlated with pACC concentration, suggesting that the UPS is still in energetic balance.
- In contrast to WT, no positive correlation was found between the chymotrypsin-like activity and the levels of $\beta 5$ -subunit in KO mice. This suggests that the alteration of proteasome activity is specific and independent of the amount of $\beta 5$ -subunit in KO mice.

4 Discussion

The goal of this thesis was to gain more insight into the role of the UPS in the pathogenesis of FHC. The work was based on former data suggesting that the UPS is not only responsible for the degradation of truncated cMyBP-C, but that mutated cMyBP-C can also cause impairment of the UPS (Sarikas et al., 2005; Bahrudin et al., 2008). These data had raised the hypothesis that cMyBP-C mutations have at least two consequences – the lack of enough wild-type protein (“haploinsufficiency”) and impairment of the UPS, e.g. by over usage or chocking by the mutated proteins. Both mechanisms could lead to cardiac hypertrophy and it would be difficult to differentiate between them in tissue from patients with FHC or in cells treated with adenovirus. Therefore, this thesis studied whether UPS alterations also exist in a model of cardiac hypertrophy associated with a complete absence of both cMyBP-C mRNA and protein. Thus, any change in the UPS would be due either to the lack of cMyBP-C (“extreme haploinsufficiency”) or indirect consequences of cardiac hypertrophy. The experiments were performed in cMyBP-C-KO that had been created by targeted deletion of the *MYBPC3* gene encoding cMyBP-C (Carrier et al., 2004). This model was also appropriate to get more insights into the mechanisms leading to FHC in humans carrying homozygous *MYBPC3* mutations that result in absence of protein.

Over the last two decades, the UPS has been increasingly recognized as a major system in several biological processes including cell proliferation, adaptation to stress and cell death. More recently, activation or impairment of the UPS has been reported in cardiac disease (for review, see Mearini et al., 2008). Particularly, accumulation of ubiquitinated proteins has been reported in human heart failure (Hein et al., 2003; Weekes et al., 2003; Tsukamoto et al., 2006; Birks et al., 2008) suggesting impaired UPS. Moreover, the UPS was altered in murine, canine or feline models of aortic banding (Okada et al., 2004; Balasubramanian et al., 2006; Depre et al., 2006; Tsukamoto et al., 2006; Sano et al., 2007) and in cardiac myocytes overexpressing truncated cMyBP-C (Sarikas et al., 2005; Bahrudin et al., 2008).

The fundamental hypotheses of our work where the following: i) cardiac hypertrophy results from lack of cMyBP-C and is associated with high steady-state-levels of ubiquitinated proteins; ii) high steady-state-levels of ubiquitinated proteins result from

UPS impairment, and iii) impairment of the UPS gives rise to misusage of ATP.

4.1 Hypothesis 1: Cardiac hypertrophy results from the absence of cMyBP-C and is associated with high steady-state levels of ubiquitinated proteins.

We evaluated the growth and development of cardiac hypertrophy as well as the levels of several cardiac-specific proteins from birth to 50 wk-old KO and WT mice. The BW of both KO and WT mice increased over the first 9 weeks and remained stable thereafter. The HW showed a similar development in both KO and WT mice. We first wanted to use CSQ as an endogenous control to normalize and compare data between the different postnatal time-points. CSQ is a high capacity Ca^{2+} -binding protein localized in the luminal side of the SR. It is involved in the Ca^{2+} homeostasis of the cardiac myocytes and interacts with the ryanodine receptor (Zhang et al., 1997). The level of CSQ simultaneously increased with BW and HW at least until the age of 13 wks (Figure 3.3), it was therefore not used to compare the different postnatal points. On the other hand, CSQ was used to compare KO and WT at each specific time-point. Similarly, the level of cMyBP-C, another cardiac-specific protein, increased during the first weeks of postnatal development (Figure 2.2). In contrast, the level of all the other analysed proteins (ubiquitinated proteins, pACC and β 5-subunit of the proteasome) decreased in the same period of time in both KO and WT mice.

The HW, but not the BW was higher after 4 wks in KO than WT mice. Therefore the higher HW/BW ratio did not result from a lower BW, but indeed from a higher HW in the KO compared to WT mice. The KO mice exhibited macroscopically apple-shaped heart and it is remarkable that their lifespan was unaffected. This is in contrast to humans with a homozygous *MYBPC3* mutation resulting in absence of cMyBP-C, which was associated with severe hypertrophic cardiomyopathy, heart failure and sudden cardiac death at the age of 9 months (Richard et al., 2003). On the other hand, these data provide evidence that cMyBP-C is not a crucial sarcomeric protein, but why do KO mice develop cardiac hypertrophy? The absence of cMyBP-C induced up-regulation of genes encoding proteins involved in energy metabolism (fatty acid metabolism), maladaptive hypertrophy (Jnk and p38 signalling pathways) and components of the UPS (E2 ubiquitin conjugating-enzyme and E3 ubiquitin ligase) in the same 9-wk-old homozygous KO mice (Eijssen et al., 2008). Interestingly, these genes were also up-regulated before the development of septal hypertrophy in the heterozygous cMyBP-C mice, which carry only one functional allele

and 25% lower amount of cMyBP-C than WT mice (Carrier et al., 2004; Eijssen et al., 2008). Moreover, in another cMyBP-C knock-in (KI) mouse developed in our group, which carries a human *MYBPC3* point mutation at the homozygous state, low amount of mutant cMyBP-C was detected (Schlossarek et al., 2006). As for the KO mice, KI mice exhibited myocyte and left ventricular hypertrophy with reduced fractional shortening and interstitial fibrosis. These lines of evidence suggest that a low amount or the absence of cMyBP-C is sufficient to activate hypertrophic pathways, but the exact mechanism remains unclear.

Whereas the HW was significantly higher already at 4 wks of age, the steady-state levels of ubiquitinated proteins were significantly higher from 6 wks on in KO compared to WT mice. Similar to KO mice, KI mice also exhibited higher amounts of ubiquitinated proteins after 6 wks of age (Sultan et al., 2007). Greater levels of ubiquitinated proteins have been described in human heart failure (Hein et al., 2003; Weekes et al., 2003; Tsukamoto et al., 2006; Birks et al., 2008). In agreement to our data, higher amount of ubiquitinated proteins were detected after the development of cardiac hypertrophy but before the development of heart failure in an experimental mouse model induced by transverse aortic constriction (Tsukamoto et al., 2006). Taken together, these data suggest that cardiac hypertrophy precedes the accumulation of ubiquitinated proteins.

During the structural changes required for cardiac hypertrophy and failure a global increase in gene expression is necessary, including re-expression of fetal genes such as β -MHC and α -skeletal actin (Boheler et al., 1991; Schwartz et al., 1992; Schwartz 1993). At least β -MHC is known to be ubiquitinated and degraded by the UPS (Fielitz et al., 2007). There is evidence that the UPS is involved in the breakdown of cardiac actin in insulin-deficient mice (Hu et al., 2008). The proteasome inhibitor bortezomib increased the level of several isoforms of MHC, including β -MHC in diaphragm of rats with chronic heart failure (van Hees et al., 2008). The higher mRNA levels of β -MHC and α -skeletal-actin previously detected in the hypertrophied KO mice (Carrier et al., 2004) could result in higher ubiquitinated β -MHC and α -skeletal-actin. However, this hypothesis was not verified by mass spectrometry in the present study, at least for MHC. Interestingly, no correlation between the degree of hypertrophy and the levels of ubiquitinated proteins was found in both KO and WT, suggesting that cardiac hypertrophy and high amount of ubiquitinated proteins are independent in KO mice. Further analyses are needed to determine whether higher ubiquitin mRNA levels are present in KO mice as shown before in chronic heart

failure and cardiac hypertrophy (van Hees et al., 2008).

A key element of cardiac hypertrophy is an acceleration of protein turnover (Depre et al., 2006). It refers to both protein synthesis and protein degradation. Interestingly, while protein synthesis has constantly been shown to be increased, protein degradation was either increased or unchanged in hypertrophic hearts, and surprisingly decreased by cardiac work or high aortic constriction in Langendorff preparations (Gordon et al., 1987; Morgan et al., 1987). Since there is evidence that protein synthesis is not directly correlated with high levels of ubiquitinated proteins in cells (Schubert et al., 2000), we hypothesized that accumulation of ubiquitinated proteins could result from UPS impairment. Indeed, inhibition of the proteasome by pharmacological means results in accumulation of ubiquitinated proteins in cardiac myocytes (Sarikas et al., 2005; Hedhli et al., 2008a). Therefore, if the UPS is blocked, proteins that are known to be degraded by the UPS should be accumulated. Components involved in hypertrophic pathways, e.g. β -catenin and calcineurin are degraded by the UPS (Glickman and Ciechanover 2002; Li et al., 2004; Wilkins et al., 2004), and could therefore contribute/increase the development of cardiac hypertrophy. We could also speculate that transcription factors that are normally degraded by the UPS could contribute to the development of cardiac hypertrophy by gain of function toxicities. In an experimental mouse model of heart failure induced by transverse aortic constriction both increased steady-state levels of ubiquitinated proteins and depression of proteasome activities (Tsukamoto et al., 2006) were described. The same model showed prolongation of ER stress characterized by accumulation of ER chaperones (Okada et al., 2004). Recent data also showed that the transcription factor p53 accumulates during the transition from cardiac hypertrophy to heart failure (Sano et al., 2007). These data are consistent with the hypothesis that removal of abnormal proteins by the proteasome is insufficient in cardiac hypertrophy and failure. In the present study, we did not find specific ubiquitinated proteins by mass spectrometry in KO hearts. We cannot exclude, however, the presence of aggregates in another protein fraction, i.e. in insoluble protein pellets that were not analysed in the present study.

4.2 Conclusion Hypothesis 1:

These data suggest that the lack of cMyBP-C is a strong trigger of cardiac hypertrophy, but does not grossly reduce survival in KO mice. Accumulation of ubiquitinated proteins is associated with the development of cardiac hypertrophy but no specific ubiquitinated

aggregates were detected in KO hearts yet. Whether accumulation of ubiquitinated proteins is the chicken or the egg of cardiac hypertrophy in KO mice cannot be fully answered by the present study though it seems to follow rather than to precede cardiac hypertrophy. On the other hand, accumulations of ubiquitinated proteins suggest impairment of the UPS in KO mice.

4.3 Hypothesis 2: High steady-state levels of ubiquitinated proteins result from impairment of the UPS.

UPS impairment is expected to be associated with aberrant protein aggregation. In neurodegenerative disorders such as Alzheimer's, Parkinson's, and Huntington's disease aberrant protein aggregates is a common pathologic process (for reviews, see Dawson and Dawson 2003; Bossy-Wetzel et al., 2004). Proteasome inhibition induced by pharmacological means or by mutant cMyBP-C was associated with ubiquitin-positive aggregates after gene transfer in cardiac myocytes (Sarikas et al., 2005). Anomalous protein aggregates were found in cardiac myocytes and tissue in human hypertrophic and dilated cardiomyopathies (Heling et al., 2000; Sanbe et al., 2004). Experimentally, involvement of the UPS in familial dilated cardiomyopathy has been mainly evidenced in desmin-related myopathy (DRM), which was initially characterized by marked accumulation of desmin in skeletal and cardiac muscle (Rappaport et al., 1988). The same group identified ten years later the corresponding R120G mutation in the gene encoding α B-crystallin (CryAB; Vicart et al., 1998). CryAB is the most abundant heat shock protein in the heart. Transgenic mice expressing a CryAB^{R120G} mutant develop cardiomyopathy at 3 months and die at 6-7 months from heart failure (Wang et al., 2001). These mice show perinuclear aggregates containing both desmin and preamyloid oligomer (Sanbe et al., 2004; Sanbe et al., 2005), suggesting that CryAB-DRM is a subclass of the aggresomal and amyloid-related disorders such as Alzheimer's and Parkinson's diseases (Sanbe et al., 2003). The cross between CryAB^{R120G} mutant transgenic mice with the GFPdgn reporter mice revealed marked UPS impairment and accumulation of aggregates (Chen et al., 2005). Interestingly, voluntary exercise slows the progression to heart failure and reduced preamyloid aggregates formation in CryAB^{R120G} mice (Maloyan et al., 2007). UPS impairment was also found in another DRM mouse model associated with a desmin mutation (Liu et al., 2006b). The molecular mechanisms by which aggregates impair the UPS remain elusive. It has been proposed that aggregated proteins themselves directly

inhibit the 26S proteasome by “chocking” the proteases. Alternatively protein aggregates may indirectly interfere with UPS function by inactivating or depleting UPS components. Data obtained by Wang and collaborators indeed suggest a diminished entry of ubiquitinated protein into the 20S proteasome, likely due to depletion of key components of the 19S proteasomes (Chen et al., 2005; Liu et al., 2006b).

Impairment of UPS is expected to be associated with decreased proteasome activities as previously observed in an experimental mouse model of cardiac hypertrophy (Tsukamoto et al., 2006). However, opposite results were obtained in the present study. Specifically, the chymotrypsin-like activity was markedly greater in KO hearts compared to WT mice. Whereas chymotrypsin-like activity was not negatively correlated to the amount of ubiquitinated proteins, it was positively correlated with the degree of hypertrophy in KO mice, suggesting that these parameters are dependent from each other. Therefore, and in contrast to our expectations, these data strongly suggest that the proteasome is rather activated in this model of cardiac hypertrophy. These data are in agreement with recent observations showing increased levels of UPS components and/or proteasome activities in murine, canine and feline models of TAC-induced cardiac hypertrophy (Balasubramanian et al., 2006; Depre et al., 2006). Similarly in different transgenic mice with cardiac hypertrophy, proteasome activities were also increased (Chen et al., 2005; Hedhli et al., 2008b). One explanation could be simply the increased protein turnover during cardiac hypertrophy, which implies increased synthesis and therefore increased degradation. However, it does not fit with accumulation of ubiquitinated proteins in KO mice. Alternatively, the greater chymotrypsin-like activity may be a compensatory mechanism to get rid of hypertrophic factors and therefore to prevent further cardiac hypertrophy in KO mice. Interestingly, the higher chymotrypsin-like activity was not associated with higher amounts of $\beta 5$ -subunit of the proteasome that carries this activity in KO mice. This contrasts to previous data showing that greater activity was associated with higher level of $\beta 5$ -subunit in different models of cardiac hypertrophy (Chen et al., 2005; Hedhli et al., 2008b; Powell et al., 2008). In one of these studies, the amount of several proteasome subunits, though not shown for the $\beta 5$ -subunit, was specifically higher in the nuclear, but not in the cytosolic fraction with hypertrophy (Hedhli et al., 2008b). In the present work, the chymotrypsin-like activity was measured in the cytosolic fraction, whereas the amount of $\beta 5$ -subunit was determined in the total protein fraction. Further analyses are needed to determine the $\beta 5$ -subunit levels in different compartments of the cardiac myocyte.

4.4 Conclusion Hypothesis 2:

In contrast to our expectations, the high steady-state levels of ubiquitinated proteins were not correlated with low, but high proteasome activity in KO mice. On the other hand, cardiac hypertrophy and chymotrypsin-like activity were positively correlated, suggesting that a greater chymotrypsin-like activity is a compensatory mechanism to get rid of hypertrophic factors and therefore to prevent further cardiac hypertrophy in KO mice.

4.5 Hypothesis 3: A compensatory increase in the main degradation activity of the proteasome leads to misuse of ATP.

Since the UPS is a highly ATP-dependent system (Powell et al., 2007), the higher steady-state level of ubiquitinated proteins and the greater proteasome activities were expected to result in ATP depletion in KO mice. The depletion of ATP was determined indirectly by quantifying the amount of pACC, which is a product of the AMP-kinase. The AMP-kinase reacts in a sensitive manner to changes of the ratio of AMP and ATP (Carling 1989); however it is not possible to convert the measurements into absolute concentrations of AMP (Hardie et al., 1999). No difference in the amounts of pACC was detected during post-natal development in KO compared to WT mice. This suggests that the cells were in energetic balance. In contrast, ATP depletion detected by ^{31}P magnetic resonance spectrometry was reported in human hearts with FHC (Cirilley et al., 2003) and in asymptomatic patients with HCM (Jung et al., 1998). However the process of ATP hydrolysis by the 26S proteasome still remains unclear. Recently, it has been shown in bovine red blood cells that ATP hydrolysis was necessary for assembly and activation of the proteasome (Liu et al., 2006a). On the other hand, the same study showed evidence that ATP was not necessary for deubiquitination of proteins resistant for degradation and for degradation of non ubiquitinated misfolded substrates (Liu et al., 2006a). Interestingly, it has also been shown that high concentrations of ATP can impair chymotrypsin-like activities in rat hearts (Powell et al., 2007).

The pACC levels were very high in neonates and dropped shortly after birth in both KO and WT mice. This suggests that the concentration of ATP is very low at birth and is strongly stimulated in the first week of life in mouse hearts. Then, the levels of pACC slightly increased between 2 and 9 wks of age and then remained stable in both KO and WT mice. This argues against a major energy deficit in KO, but clearly more work is

needed to elucidate this question with more sensitive methods.

4.6 Conclusion hypothesis 3:

Taken together the hypothesis of UPS impairment contributing to misuse of ATP could not be substantiated. Greater chymotrypsin-like activities in the KO did not lead to higher pACC levels and were likely not due to increased $\beta 5$ levels.

4.7 Possible overview

The absence of cMyBP-C leads to incomplete relaxation of intact cardiac myocytes in diastole (Pohlmann et al., 2007) and impaired diastolic function *in vivo* (Carrier et al., 2004). The impaired diastolic function was also detected in other mouse models of FHC overexpressing two different mutations in the myosin light chain gene (Abraham et al., 2009). These data indicate that mouse models with human sarcomeric gene mutations reproduce hypertrophy and diastolic dysfunction, which are hallmarks of human FHC.

We could hypothesize that impaired diastolic function is the trigger of cardiac hypertrophy (Figure 4.4). Cardiac hypertrophy requires an increase in protein turnover in individual cardiac myocytes that result from the synthesis of *de novo* proteins exceeding protein degradation. This could have two consequences. On the one hand, it could result in higher amount of ubiquitinated proteins. On the other hand if the UPS is impaired, factors promoting cardiac hypertrophy are degraded with delay. Thus the UPS machinery reacts with a compensatory stronger performance of the chymotrypsin-like activity. Additionally, age related proteasome depletion (Bulteau et al., 2002) could further strengthen insufficient compensatory mechanisms. This suggest that the UPS might provide and promote a *circulus vitiosus*, which finally through accumulation of ubiquitinated proteins could lead, because of deficient compensatory mechanisms to hypertrophic cardiomyopathy (Figure 4.1).

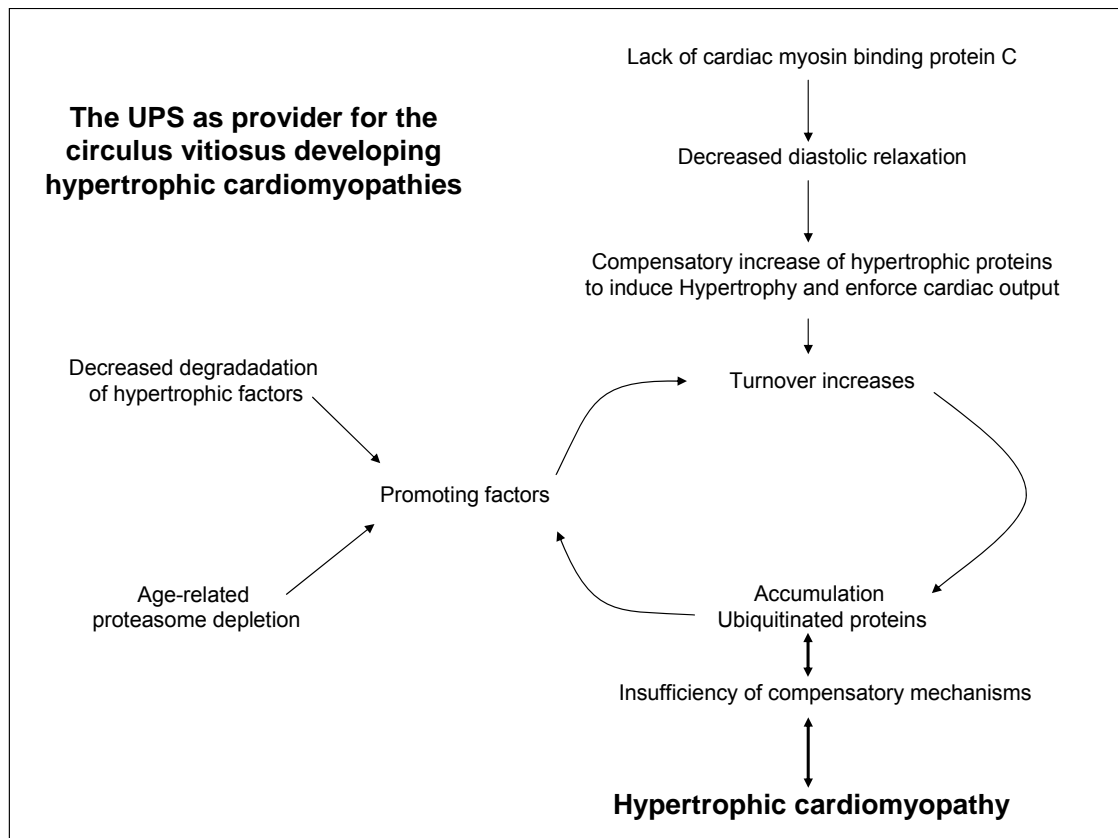


Figure 4.1: A model of the pathomechanism of hypertrophic cardiomyopathy.

The illustration shows a potential evolution of FHC based on the null-allele hypothesis with the UPS as provider for the development of FHC.

4.8 Outlook

Immunofluorescence of KO cardiac myocytes or cardiac sections could be useful to investigate whether aggresomes or accumulation of ubiquitinated-proteins with age alters the UPS machinery and consequently leads to cardiac hypertrophy.

It would be interesting to compare KI and KO mice with there corresponding littermates after physical exercise to evaluate whether there is an earlier onset of increased ubiquitinated proteins caused by greater protein turnover. In the same study it could be investigated if there is an increased risk of sudden death in the hypertrophic mice.

Further analyses are needed to evaluate whether the $\beta 5$ -subunit of the proteasome, and therefore the 26S proteasome itself is translocated in specific compartments of cardiac myocytes in pathological conditions and after physical stress.

Since KO mice exhibited greater chymotrypsin-like activity, which is positively correlated to the degree of cardiac hypertrophy, *in vivo* treatment of mice with proteasome inhibitor could attenuate or reverse the development of cardiac hypertrophy in KO mice. Indeed, in a recent study 1-wk *in vivo* injection of the proteasome inhibitor epoxomicin was shown to prevent TAC-induced hypertrophy in mice (Depre et al., 2006). More recently, the same group showed that epoxomicin can reverse stable and chronic cardiac hypertrophy in transgenic mice overexpressing the heat shock protein Hsp22 (Hedhli et al., 2008a). Epoxomicin is an irreversible inhibitor of the chymotrypsin-like activity of the proteasome, which only inhibits 30 – 40 % of the overall proteasome activity. This potentially limits the adverse effect on the myocytes. In comparison to banded mice without treatment, the animals after one week of “therapy” showed reduced cell size, reduced apoptosis, stabilization of ejection fraction and no signs of heart failure. These experiments were performed under short-term conditions and further studies will be necessary to investigate long-term and possible adverse effects of the treatment. In the same study the underlying effect of the treatment with epoxomicin was attributed to an inhibition of the transcription factor NF- κ B pathway mediating an accumulation of interstitial collagen and further cardiac remodelling.

5 Abstract

Mutations in the cardiac myosin-binding protein C (cMyBP-C) gene are frequently involved in familial hypertrophic cardiomyopathy. The work was based on former data suggesting that the ubiquitin-proteasome system (UPS) is not only responsible for the degradation of truncated cMyBP-C, but that mutated cMyBP-C can also cause impairment of the UPS. These data had raised the hypothesis that cMyBP-C mutations have at least two consequences – the lack of enough wild-type protein (“haploinsufficiency”) and impairment of the UPS. This thesis studied whether UPS alterations also exist in a model of cardiac hypertrophy associated with a complete absence of both cMyBP-C mRNA and protein. Thus, the change in the UPS could either be due to the lack of cMyBP-C (“extreme haploinsufficiency”) or to indirect consequences of cardiac hypertrophy.

The experiments were performed in cMyBP-C-KO mice that had been created by targeted deletion of the *MYBPC3* gene encoding cMyBP-C. We studied myocardial tissues of cMyBP-C-KO mice at different postnatal time points (birth to 50 wks) and compared them to age-matched wild-type (WT) mice (n=5-8 in each group). The steady state levels of ubiquitinated proteins were determined by Western-blot analyses. In both groups, the ubiquitinated protein amount dropped after birth. Compared to WT levels ubiquitinated proteins were up to 122% higher in KO mice. The chymotrypsin-like activity of the proteasome was measured with the specific SUC-LLVY-AMC fluorogenic substrate. The difference in chymotrypsin-like activity between KO and WT was 0 at birth and then increased to >50% at 6 wks.

The chymotrypsin-like activity was positively correlated with the degree of hypertrophy in KO (Spearman $r=0.39$, $P<0.01$), but not with ubiquitinated protein levels. To determine whether the higher chymotrypsin-like activity results from higher levels of the protein carrying this activity we determined the concentration of the $\beta 5$ -subunit of the 20S proteasome. The levels of $\beta 5$ -subunit dropped at a similar rate shortly after birth in both WT and KO. To investigate whether the higher UPS activity in KO is associated with increased ATP usage and therefore increased AMP-kinase activity, the concentration of phosphorylated acetyl-CoA carboxylase (pACC) was determined by Western-blot. The pACC level decreased after birth at exactly the same rate in both mouse lines. In summary, this work shows that i) the UPS is altered in KO at different postnatal time points, ii) the chymotrypsin-like activity increases with the degree of hypertrophy. These data suggest that i) UPS alterations are a common remodeling mechanism associated with cardiac hypertrophy and can occur in the absence of cMyBP-C and ii) the higher chymotrypsin-like activity is likely a compensatory mechanism against further development of hypertrophy.

6 Zusammenfassung

Veränderungen des Ubiquitin-Proteasom Systems in cMyBP-C *knockout* Mäusen

Mutationen im kardialen Myosin-bindenden Protein C (cMyBP-C) Gen sind ein häufiger Grund für die hypertrophe Kardiomyopathie. Die vorliegende Arbeit baut auf Veröffentlichungen auf, die zu dem Ergebnis kamen, dass das Ubiquitin Proteasom System (UPS) nicht nur für den Abbau mutierter cMyBP-C Varianten verantwortlich ist, sondern dass Letztere auch das UPS beeinträchtigen können. Demnach hätten Mutationen von cMyBP-C mindestens zwei Auswirkungen: einen Mangel an Wildtyp (WT) cMyBP-C („Haploinsuffizienz“) und eine Beeinträchtigung des UPS. In dieser Arbeit wurde untersucht, ob Veränderungen des UPS auch in einem Herzhypertrophiemodell ohne cMyBP-C mRNA und Protein bestehen. In diesem Fall wäre jegliche Änderung im UPS entweder als Folge des Fehlens von cMyBP-C („extreme Haploinsuffizienz“) oder als indirekte Folge einer Herzhypertrophie anzusehen.

Die Versuche wurden mit cMyBP-C-KO Mäusen durchgeführt, welche durch gezielte Deletion des *MYBPC3* Gens, das für cMyBP-C kodiert, geschaffen worden waren. Herzgewebe von cMyBP-C-KO Mäusen unterschiedlichen Alters (Geburt – 50 Wochen) wurde mit Herzgewebe der zugehörigen WT Mäusen (n=5-8 pro Gruppe) gleichen Alters verglichen. Die Werte der sich im Fließgleichgewicht befindlichen ubiquitinierten Proteine wurden mit Western Blots bestimmt. In beiden Gruppen fielen die Werte der ubiquitinierten Proteine nach der Geburt ab. Im Vergleich zu den Werten bei den WT waren die ubiquitinierten Proteine in den KO Mäusen bis zu 122% höher. Die Chymotrypsin-ähnliche Aktivität des Proteasoms wurde mit Hilfe des spezifischen fluoreszenz erzeugenden Substrates SUC-LLVY-AMC gemessen. Sie war bei KO und WT zum Zeitpunkt der Geburt gleich hoch, nahm jedoch in den darauffolgenden sechs Wochen bei KO um mehr als 50% stärker zu als bei WT. Bei den KO war die Chymotrypsin-ähnliche Aktivität mit dem Ausmaß der Herzhypertrophie korreliert (Spearman $r=0.39$, $P<0.01$), die Werte der ubiquitinierten Proteine hingegen nicht. Um festzustellen, ob die höhere Chymotrypsin-ähnliche Aktivität Folge eines Anstieges des Proteins ist, welches diese Aktivität trägt, wurde die Konzentration der $\beta 5$ -Untereinheit des 20S Proteasoms bestimmt. Die Werte der $\beta 5$ -Untereinheit nahmen kurz nach der Geburt in ähnlichem Ausmaße sowohl bei WT als auch bei KO Mäusen ab. Um zu erforschen, ob die höhere UPS-Aktivität mit erhöhtem ATP-Verbrauch und darauffolgend mit erhöhter AMP-Kinase-Aktivität einhergeht, wurde die Konzentration der phosphorylierten Acetyl-CoA Carboxylase (pACC) per Western Blot ermittelt. Die Werte der pACC fielen kurz nach der Geburt ab. KO und WT unterschieden sich nicht.

Zusammengefasst zeigt diese Arbeit Veränderungen des UPS bei cMyBP-C-KO zu verschiedenen postnatalen Zeitpunkten, die im Fall der Chymotrypsin-ähnlichen Aktivität mit dem Ausmaß der Herzhypertrophie korreliert waren. Dies deutet auf Folgendes hin: i) UPS-Veränderungen stellen einen gebräuchlichen Umbaumechanismus bei Herzhypertrophie dar und können auch in Abwesenheit von cMyBP-C-Mutanten auftreten. ii) Die höhere Chymotrypsin-ähnliche Aktivität ist wahrscheinlich ein Kompensationsmechanismus gegen zunehmende Herzhypertrophie.

7 References

- Abraham, T.P., Jones, M., Kazmierczak, K., Liang, H.-Y., Pinheiro, A.C., Wagg, C.S., Lopaschuk, G.D., and Szczesna-Cordary, D. (2009) Diastolic Dysfunction in Familial Hypertrophic Cardiomyopathy Transgenic Model Mice. *Cardiovasc Res* cvp016.
- Alcalai, R., Seidman, J.G., and Seidman, C.E. (2008) Genetic basis of hypertrophic cardiomyopathy: from bench to the clinics. *J Cardiovasc Electrophysiol* 19, 104-10.
- Alyonycheva, T., Cohen-Gould, L., Siewert, C., Fishman, D.A., and Mikawa, T. (1997) Skeletal muscle-specific myosin binding protein-H is expressed in Purkinje fibers of the cardiac conduction system. *Circ. Res.* 80, 665-672.
- Bahrudin, U., Morisaki, H., Morisaki, T., Ninomiya, H., Higaki, K., Nanba, E., Igawa, O., Takashima, S., Mizuta, E., Miake, J., Yamamoto, Y., Shirayoshi, Y., Kitakaze, M., Carrier, L., and Hisatome, I. (2008) Ubiquitin-proteasome system impairment caused by a missense cardiac myosin-binding protein C mutation and associated with cardiac dysfunction in hypertrophic cardiomyopathy. *J Mol Biol* 384, 896-907.
- Balasubramanian, S., Mani, S., Shiraishi, H., Johnston, R.K., Yamane, K., Willey, C.D., Cooper IV, G., Tuxworth, W.J., and Kuppuswamy, D. (2006) Enhanced ubiquitination of cytoskeletal proteins in pressure overloaded myocardium is accompanied by changes in specific E3 ligases. *Journal of Molecular and Cellular Cardiology* 41, 669-679.
- Birks, E.J., Latif, N., Enesa, K., Folkvang, T., Luong le, A., Sarathchandra, P., Khan, M., Ova, H., Terracciano, C.M., Barton, P.J., Yacoub, M.H., and Evans, P.C. (2008) Elevated p53 expression is associated with dysregulation of the ubiquitin-proteasome system in dilated cardiomyopathy. *Cardiovasc Res* 79, 472-80.
- Boheler, K.R., Carrier, L., Chassagne, C., de la Bastie, D., Mercadier, J.J., and Schwartz, K. (1991) Regulation of myosin heavy chain and actin isogenes expression during cardiac growth. *Mol Cell Biochem* 104, 101-7.
- Bonne, G., Carrier, L., Bercovici, J., Cruaud, C., Richard, P., Hainque, B., Gautel, M., Labeit, S., James, M., Beckmann, J.S., Weissenbach, J., Vosberg, H.P., Fiszman, M., Komajda, M., and Schwartz, K. (1995) Cardiac myosin binding protein-C gene splice acceptor site mutation is associated with familial hypertrophic cardiomyopathy. *Nature Genet* 11, 438-440.
- Bossy-Wetzell, E., Schwarzenbacher, R., and Lipton, S.A. (2004) Molecular pathways to neurodegeneration. *Nat Med* 10 Suppl, S2-9.

- Bottinelli, R., Coviello, D.A., Redwood, C.S., Pellegrino, M.A., Maron, B.J., Spirito, P., Watkins, H., and Reggiani, C. (1998) A mutant tropomyosin that causes hypertrophic cardiomyopathy is expressed in vivo and associated with an increased calcium sensitivity. *Circ. Res.* 82, 106-115.
- Bradford, M.M. (1976) A rapid and sensitive method for the quantitation of microgram quantities of protein utilizing the principle of protein-dye binding. *Anal Biochem* 72, 248-54.
- Braunwald, E., Ross, J., Jr., and Sonnenblick, E.H. 1976. Mechanisms of contraction of the normal and failing heart. Boston: Little, Brown and Co.
- Brenner, B. 2005. Muskulatur. In: Klinke R., Pape H.-C., Silbernagl S., editors. *Physiologie*. Fifth ed. Stuttgart: Georg Thieme Verlag. p 103-133.
- Bulteau, A.L., Szweda, L.I., and Friguet, B. (2002) Age-dependent declines in proteasome activity in the heart. *Arch Biochem Biophys* 397, 298-304.
- Cabin. 1992. The Heart and Circulation. In: Zarret B M.M., Cohen L, editor. Yale University School of Medicine Heart Book. First ed. New York.
- Carling, D., Paul R. CLARKE, Victor A. ZAMMIT, D. Grahame HARDIE., (1989) Purification and characterization of the AMP-activated protein kinase. *European Journal of Biochemistry* 186, 129-136.
- Carrier, L., Bonne, G., Bährend, E., Yu, B., Richard, P., Niel, F., Hainque, B., Cruaud, C., Gary, F., Labeit, S., Bouhour, J.B., Dubourg, O., Desnos, M., Hagege, A.A., Trent, R.J., Komajda, M., and Schwartz, K. (1997) Organization and sequence of human cardiac myosin binding protein C gene (*MYBPC3*) and identification of mutations predicted to produce truncated proteins in familial hypertrophic cardiomyopathy. *Circ Res* 80, 427-434.
- Carrier, L., Hengstenberg, C., Beckmann, J.S., Guicheney, P., Dufour, C., Bercovici, J., Dausse, E., Berebbi-Bertrand, I., Wisnewsky C, Pulvenis, D., Fetler, L., Vignal, A., Weissenbach, J., Hillaire, D., Feingold, J., Bouhour, J.B., Hagege, A., Desnos, M., Isnard, R., Dubourg, O., Komajda, M., and Schwartz, K. (1993) Mapping of a novel gene for familial hypertrophic cardiomyopathy to chromosome 11. *Nature Genet.* 4, 311-313.
- Carrier, L., Knoell, R., Vignier, N., Keller, D.I., Bausero, P., Prudhon, B., Isnard, R., Ambroisine, M.L., Fiszman, M., Ross, J., Jr., Schwartz, K., and Chien, K.R. (2004) Asymmetric septal hypertrophy in heterozygous cMyBP-C null mice. *Cardiovasc Res* 63, 293-304.
- Chen, Q., Liu, J.B., Horak, K.M., Zheng, H., Kumarapeli, A.R., Li, J., Li, F., Gerdes, A.M., Wawrousek, E.F., and Wang, X. (2005) Intracellular amyloidosis impairs proteolytic function of proteasomes in cardiomyocytes by compromising substrate uptake. *Circ Res* 97, 1018-26.

- Ciechanover, A. (2006) The ubiquitin proteolytic system: from a vague idea, through basic mechanisms, and onto human diseases and drug targeting. *Neurology* 66, S7-19.
- Craig, R., and Offer, G. (1976) The localization of C-protein in rabbit skeletal muscle. *Proc. Royal. Soc. Lond. B*192, 451-454.
- Crilley, J.G., Boehm, E.A., Blair, E., Rajagopalan, B., Blamire, A.M., Styles, P., McKenna, W.J., Ostman-Smith, I., Clarke, K., and Watkins, H. (2003) Hypertrophic cardiomyopathy due to sarcomeric gene mutations is characterized by impaired energy metabolism irrespective of the degree of hypertrophy. *J Am Coll Cardiol* 41, 1776-82.
- Cuda, G., Fananapazir, L., Zhu, W.S., Seller, J.R., and Epstein, N.E. (1993) Skeletal muscle expression and abnormal function of β -myosin in hypertrophic cardiomyopathy. *J. Clin. Invest.* 91, 2861-2865.
- Dawson, T.M., and Dawson, V.L. (2003) Molecular Pathways of Neurodegeneration in Parkinson's Disease
10.1126/science.1087753. *Science* 302, 819-822.
- Depre, C., Wang, Q., Yan, L., Hedhli, N., Peter, P., Chen, L., Hong, C., Hittinger, L., Ghaleh, B., Sadoshima, J., Vatner, D.E., Vatner, S.F., and Madura, K. (2006) Activation of the cardiac proteasome during pressure overload promotes ventricular hypertrophy. *Circulation* 114, 1821-8.
- Eijssen, L.M., van den Bosch, B.J., Vignier, N., Lindsey, P.J., van den Burg, C.M., Carrier, L., Doevendans, P.A., van der Vusse, G.J., and Smeets, H.J. (2008) Altered myocardial gene expression reveals possible maladaptive processes in heterozygous and homozygous cardiac myosin-binding protein C knockout mice. *Genomics* 91, 52-60.
- Fielitz, J., Kim, M.S., Shelton, J.M., Latif, S., Spencer, J.A., Glass, D.J., Richardson, J.A., Bassel-Duby, R., and Olson, E.N. (2007) Myosin accumulation and striated muscle myopathy result from the loss of muscle RING finger 1 and 3. *J Clin Invest* 117, 2486-2495.
- Flashman, E., Redwood, C., Moolman-Smook, J., and Watkins, H. (2004) Cardiac myosin binding protein C: its role in physiology and disease. *Circ Res* 94, 1279-89.
- Freiburg, A., and Gautel, M. (1996) A molecular map of the interactions between titin and myosin-binding protein C. Implications for sarcomeric assembly in familial hypertrophic cardiomyopathy. *Eur J Biochem* 235, 317-326.
- Geisterfer-Lowrance, A.A., Kass, S., Tanigawa, G., Vosberg, H.P., McKenna, W., Seidman, C.E., and Seidman, J.G. (1990) A molecular basis for familial hypertrophic cardiomyopathy: a β cardiac myosin heavy chain gene missense mutation. *Cell* 62, 999-1006.
- Glickman, M.H., and Ciechanover, A. (2002) The ubiquitin-proteasome proteolytic pathway: destruction for the sake of construction. *Physiol Rev* 82, 373-428.

- Goldberg, A.L. (2003) Protein degradation and protection against misfolded or damaged proteins. *Nature* 426, 895-9.
- Gordon, E.E., Kira, Y., and Morgan, H.E. (1987) Aortic perfusion pressure, protein synthesis, and protein degradation. *Circulation* 75, 178-80.
- Hardie, D.G., Salt, I.P., Hawley, S.A., and Davies, S.P. (1999) AMP-activated protein kinase: an ultrasensitive system for monitoring cellular energy charge. *Biochem J* 338 (Pt 3), 717-22.
- Hedhli, N., Lizano, P., Hong, C., Fritzky, L.F., Dhar, S.K., Liu, H., Tian, Y., Gao, S., Madura, K., Vatner, S.F., and Depre, C. (2008a) Proteasome inhibition decreases cardiac remodeling after initiation of pressure overload. *Am J Physiol Heart Circ Physiol*.
- Hedhli, N., Wang, L., Wang, Q., Rashed, E., Tian, Y., Sui, X., Madura, K., and Depre, C. (2008b) Proteasome activation during cardiac hypertrophy by the chaperone H11 Kinase/Hsp22. *Cardiovasc Res* 77, 497-505.
- Hein, S., Arnon, E., Kostin, S., Schonburg, M., Elsasser, A., Polyakova, V., Bauer, E.P., Klovekorn, W.P., and Schaper, J. (2003) Progression from compensated hypertrophy to failure in the pressure-overloaded human heart: structural deterioration and compensatory mechanisms. *Circulation* 107, 984-91.
- Heling, A., Zimmermann, R., Kostin, S., Maeno, Y., Hein, S., Devaux, B., Bauer, E., Klövekorn, W.P., Schlepper, M., Schaper, W., and Schaper, J. (2000) Increased expression of cytoskeletal, linkage, and extracellular proteins in failing human myocardium. *Circ. Res.* 86, 846-853.
- Hershko, A., and Ciechanover, A. (1982) Mechanisms of Intracellular Protein Breakdown doi:10.1146/annurev.bi.51.070182.002003. *Annual Review of Biochemistry* 51, 335-364.
- Hu, J., Klein, J.D., Du, J., and Wang, X.H. (2008) Cardiac Muscle Protein Catabolism in Diabetes Mellitus: Activation of the Ubiquitin-Proteasome System by Insulin Deficiency 10.1210/en.2008-0132. *Endocrinology* 149, 5384-5390.
- Jung, W.-I., Sieverding, L., Breuer, J., Hoess, T., Widmaier, S., Schmidt, O., Bunse, M., van Erckelens, F., Apitz, J., Lutz, O., and Dietze, G.J. (1998) 31P NMR Spectroscopy Detects Metabolic Abnormalities in Asymptomatic Patients With Hypertrophic Cardiomyopathy. *Circulation* 97, 2536-2542.
- Kamisago, M., Sharma, S.D., DePalma, S.R., Solomon, S., Sharma, P., McDonough, B., Smoot, L., Mullen, M.P., Woolf, P.K., Wigle, E.D., Seidman, J.G., Seidman, C.E., Jarcho, J., and Shapiro, L.R. (2000) Mutations in Sarcomere Protein Genes as a Cause of Dilated Cardiomyopathy. *N. Engl. J. Med.* 343, 1688-1696.

- Li, H.H., Kedar, V., Zhang, C., McDonough, H., Arya, R., Wang, D.Z., and Patterson, C. (2004) Atrogin-1/muscle atrophy F-box inhibits calcineurin-dependent cardiac hypertrophy by participating in an SCF ubiquitin ligase complex. *J Clin Invest* 114, 1058-71.
- Lim, K.L., and Tan, J.M. (2007) Role of the ubiquitin proteasome system in Parkinson's disease. *BMC Biochem* 8 Suppl 1, S13.
- Liu, C.-W., Li, X., Thompson, D., Wooding, K., Chang, T.-l., Tang, Z., Yu, H., Thomas, P.J., and DeMartino, G.N. (2006a) ATP Binding and ATP Hydrolysis Play Distinct Roles in the Function of 26S Proteasome. *Molecular Cell* 24, 39-50.
- Liu, J., Chen, Q., Huang, W., Horak, K.M., Zheng, H., Mestrl, R., and Wang, X. (2006b) Impairment of the ubiquitin-proteasome system in desminopathy mouse hearts. *Faseb J* 20, 362-4.
- Ludwig, A., Friedel, B., Metzkw, S., Meiners, S., Stangl, V., Baumann, G., and Stangl, K. (2005) Effect of statins on the proteasomal activity in mammalian endothelial and vascular smooth muscle cells. *Biochem Pharmacol* 70, 520-6.
- Maloyan, A., Gulick, J., Glabe, C.G., Kaye, R., and Robbins, J. (2007) Exercise reverses preamyloid oligomer and prolongs survival in alphaB-crystallin-based desmin-related cardiomyopathy. *Proc Natl Acad Sci U S A* 104, 5995-6000.
- Maron, B.J. (2002) Hypertrophic cardiomyopathy: a systematic review. *Jama* 287, 1308-20.
- Maron, B.J., Casey, S.A., Poliac, L.C., Gohman, T.E., Almquist, A.K., and Aeppli, D.M. (1999) Clinical course of hypertrophic cardiomyopathy in a regional United States cohort. *JAMA* 281, 650-655.
- Maron, B.J., Gardin, J.M., Flack, J.M., Gidding, S.S., Kurosaki, T.T., and Bild, D.E. (1995) Prevalence of hypertrophic cardiomyopathy in a general population of young adults: echocardiographic analysis of 4111 subjects in the CARDIA study. *Circulation* 92, 785-789.
- Mearini, G., Schlossarek, S., Willis, M.S., and Carrier, L. (2008) The ubiquitin-proteasome system in cardiac dysfunction. *Biochim Biophys Acta* 1782, 749-63.
- Mitch, W.E., and Goldberg, A.L. (1996) Mechanisms of muscle wasting. The role of the ubiquitin-proteasome pathway. *N Engl J Med* 335, 1897-905.
- Moolman, J.A., Reith, S., Uhl, K., Bailey, S., Gautel, M., Jeschke, B., Fisher, C., Ochs, J., McKenna, W.J., Klues, H., and Vosberg, H.P. (2000) A newly created splice donor site in exon 25 of the MyBP-C gene is responsible for inherited hypertrophic cardiomyopathy with incomplete disease penetrance. *Circulation* 101, 1396-1402.

- Morgan, H.E., Gordon, E.E., Kira, Y., Chua, B.H.L., Russo, L.A., Peterson, C.J., McDermott, P.J., and Watson, P.A. (1987) Biochemical Mechanisms of Cardiac Hypertrophy
doi:10.1146/annurev.ph.49.030187.002533. *Annual Review of Physiology* 49, 533-543.
- Offer, G., Moos, C., and Starr, R. (1973) A new protein of the thick filaments of vertebrate skeletal myofibrils: extraction, purification and characterization. *J. Mol. Biol.* 74, 653-676.
- Okada, K., Minamino, T., Tsukamoto, Y., Liao, Y., Tsukamoto, O., Takashima, S., Hirata, A., Fujita, M., Nagamachi, Y., Nakatani, T., Yutani, C., Ozawa, K., Ogawa, S., Tomoike, H., Hori, M., and Kitakaze, M. (2004) Prolonged endoplasmic reticulum stress in hypertrophic and failing heart after aortic constriction: possible contribution of endoplasmic reticulum stress to cardiac myocyte apoptosis. *Circulation* 110, 705-12.
- Opie, L.H., and Solaro, R.J. 2004. Myocardial contraction and relaxation. In: Opie L.H., editor. *Heart Physiology: From cell to circulation*. Philadelphia, PA: Lippincott Williams & Wilkins. p 221-246.
- Patterson, C., Ike, C., Willis, P.W.t., Stouffer, G.A., and Willis, M.S. (2007) The bitter end: the ubiquitin-proteasome system and cardiac dysfunction. *Circulation* 115, 1456-63.
- Pohlmann, L., Kroger, I., Vignier, N., Schlossarek, S., Kramer, E., Coirault, C., Sultan, K.R., El-Armouche, A., Winegrad, S., Eschenhagen, T., and Carrier, L. (2007) Cardiac myosin-binding protein C is required for complete relaxation in intact myocytes. *Circ Res* 101, 928-38.
- Powell, S.R., Davies, K.J., and Divald, A. (2007) Optimal determination of heart tissue 26S-proteasome activity requires maximal stimulating ATP concentrations. *J Mol Cell Cardiol* 42, 265-9.
- Powell, S.R., Samuel, S.M., Wang, P., Divald, A., Thirunavukkarasu, M., Koneru, S., Wang, X., and Maulik, N. (2008) Upregulation of myocardial 11S-activated proteasome in experimental hyperglycemia. *Journal of Molecular and Cellular Cardiology* 44, 618-621.
- Rappaport, L., Contard, F., Samuel, J.L., Delcayre, C., Marotte, F., Tome, F., and Fardeau, M. (1988) Storage of phosphorylated desmin in a familial myopathy. *FEBS Lett* 231, 421-5.
- Richard, P., Charron, P., Carrier, L., Ledeuil, C., Cheav, T., Pichereau, C., Benaiche, A., Isnard, R., Dubourg, O., Burbano, M., Gueffet, J.P., Millaire, A., Desnos, M., Schwartz, K., Hainque, B., and Komajda, M. (2003) Hypertrophic Cardiomyopathy: Distribution of disease genes, spectrum of mutations and implications for molecular diagnosis strategy. *Circulation* 107, 2227-2232.

- Richard, P., Villard, E., Charron, P., and Isnard, R. (2006) The genetic bases of cardiomyopathies. *J Am Coll Cardiol* 48, A79-89.
- Richardson, P., McKenna, W., Bristow, M., Maish, B., Mautner, B., O'Connell, J., Olsen, E., Thiene, G., Goodwin, J., Gyarfás, I., Martin, I., and Nordet, P. (1996) Report of the 1995 World Health Organisation/International Society and Federation of Cardiology task force on the definition and classification of cardiomyopathies. *Circulation* 93, 841-842.
- Rottbauer, W., Gautel, M., Zehelein, J., Labeit, S., Franz, W.M., Fischer, C., Vollrath, B., Mall, G., Dietz, R., Kübler, W., and Katus, H.A. (1997) Novel splice donor site mutation in the cardiac myosin-binding protein-C gene in familial hypertrophic cardiomyopathy. Characterization of cardiac transcript and protein. *J Clin Invest* 100, 475-482.
- Sanbe, A., Gulick, J., Hanks, M.C., Liang, Q., Osinska, H., and Robbins, J. (2003) Reengineering inducible cardiac-specific transgenesis with an attenuated myosin heavy chain promoter. *Circ Res* 92, 609-16.
- Sanbe, A., Osinska, H., Saffitz, J.E., Glabe, C.G., Kaye, R., Maloyan, A., and Robbins, J. (2004) Desmin-related cardiomyopathy in transgenic mice: a cardiac amyloidosis. *Proc Natl Acad Sci U S A* 101, 10132-6.
- Sanbe, A., Osinska, H., Villa, C., Gulick, J., Klevitsky, R., Glabe, C.G., Kaye, R., and Robbins, J. (2005) Reversal of amyloid-induced heart disease in desmin-related cardiomyopathy. *Proc Natl Acad Sci U S A* 102, 13592-7.
- Sano, M., Minamino, T., Toko, H., Miyauchi, H., Orimo, M., Qin, Y., Akazawa, H., Tateno, K., Kayama, Y., Harada, M., Shimizu, I., Asahara, T., Hamada, H., Tomita, S., Molkenstein, J.D., Zou, Y., and Komuro, I. (2007) p53-induced inhibition of Hif-1 causes cardiac dysfunction during pressure overload. *Nature* 446, 444-8.
- Sarikas, A., Carrier, L., Schenke, C., Doll, D., Flavigny, J., Lindenberg, K.S., Eschenhagen, T., and Zolk, O. (2005) Impairment of the ubiquitin-proteasome system by truncated cardiac myosin binding protein C mutants. *Cardiovasc Res* 66, 33-44.
- Schlossarek, S., Vignier, N., Sultan, K., Krämer, E., Mearini, G., Eschenhagen, T., and Carrier, L. (2006) Evidence of alterations of the ubiquitin-proteasome system in mouse models of familial hypertrophic cardiomyopathy. *Circulation* 114 [Suppl. II], 166.
- Schubert, U., Anton, L.C., Gibbs, J., Norbury, C.C., Yewdell, J.W., and Bannister, J.R. (2000) Rapid degradation of a large fraction of newly synthesized proteins by proteasomes. *Nature* 404, 770-4.
- Schwartz, K. (1993) Cardiomyopathies : une révolution. *Gazette Médicale* 100, 8.

- Schwartz, K., Boheler, K.R., de la Bastie, D., Lompre, A.M., and Mercadier, J.J. (1992) Switches in cardiac muscle gene expression as a result of pressure and volume overload. *Am J Physiol* 262, R364-9.
- Silbernagl, S., and Despopoulos, A. 2007. Nerv und Muskel, Arbeit. In: Silbernagl S., Despopoulos A., editors. *Taschenatlas der Physiologie*. 7th ed. Stuttgart: Georg Thieme Verlag. p 60-63.
- Sultan, K., Schlossarek, S., Englmann, D., Vignier, N., Eschenhagen, T., and Carrier, L. (2007) Alterations of the ubiquitin-proteasome system in cardiomyopathic cMyBP-C mice. *J Mol Cell Cardiol* 42, S167.
- Taylor, R., Tassy, C., Briand, M., Robert, N., Briand, Y., and Ouali, A. (1995) Proteolytic activity of proteasome on myofibrillar structures. *Molecular Biology Reports* Volume 21.
- Tsukamoto, O., Minamino, T., Okada, K., Shintani, Y., Takashima, S., Kato, H., Liao, Y., Okazaki, H., Asai, M., Hirata, A., Fujita, M., Asano, Y., Yamazaki, S., Asanuma, H., Hori, M., and Kitakaze, M. (2006) Depression of proteasome activities during the progression of cardiac dysfunction in pressure-overloaded heart of mice. *Biochem Biophys Res Commun* 340, 1125-33.
- Uhlir, N. 2005. Zytologie. In: Uhlir N., editor. *Kurzlehrbuch Histologie*. 2nd ed. Stuttgart: Georg Thieme Verlag. p 13.
- Van Dijk, S.J., Dooijes, D., dos Remedios, C., Michels, M., Lamers, J.M.J., Winegrad, S., Schlossarek, S., Carrier, L., ten Cate, F.J., Sienen, G.J.M., and van der Velden, J. (2009) Cardiac myosin-binding protein C mutations and hypertrophic cardiomyopathy: haploinsufficiency, deranged phosphorylation and cardiomyocyte dysfunction. *Circulation* 119, 1473-1483.
- van Hees, H.W.H., Li, Y.-P., Ottenheijm, C.A.C., Jin, B., Pigmans, C.J.C., Linkels, M., Dekhuijzen, P.N.R., and Heunks, L.M.A. (2008) Proteasome inhibition improves diaphragm function in congestive heart failure rats
10.1152/ajplung.00035.2008. *Am J Physiol Lung Cell Mol Physiol* 294, L1260-1268.
- Vicart, P., Caron, A., Guicheney, P., Li, Z., Prevost, M.-C., Faure, A., Chateau, D., Chapon, F., Tome, F., Dupret, J.-M., Paulin, D., and Fardeau, M. (1998) A missense mutation in the [agr]B-crystallin chaperone gene causes a desmin-related myopathy. *Hum Mol Genet* 7, 92-95.
- Wang, X., Osinska, H., Klevitsky, R., Gerdes, A.M., Nieman, M., Lorenz, J., Hewett, T., and Robbins, J. (2001) Expression of R120G- α B-Crystallin Causes Aberrant Desmin and α B-Crystallin Aggregation and Cardiomyopathy in Mice
10.1161/hh1301.092688. *Circ Res* 89, 84-91.
- Weekes, J., Morrison, K., Mullen, A., Wait, R., Barton, P., and Dunn, M.J. (2003) Hyperubiquitination of proteins in dilated cardiomyopathy. *Proteomics* 3, 208-16.

- Wilkins, B.J., Dai, Y.-S., Bueno, O.F., Parsons, S.A., Xu, J., Plank, D.M., Jones, F., Kimball, T.R., and Molkenin, J.D. (2004) Calcineurin/NFAT Coupling Participates in Pathological, but not Physiological, Cardiac Hypertrophy
10.1161/01.RES.0000109415.17511.18. *Circ Res* 94, 110-118.
- Yang, Q., Sanbe, A., Osinska, H., Hewett, T.E., Klevitsky, R., and Robbins, J. (1998) A mouse model of myosin binding protein C human familial hypertrophic cardiomyopathy. *J. Clin. Invest.* 102, 1292-1300.
- Zhang, L., Kelley, J., Schmeisser, G., Kobayashi, Y.M., and Jones, L.R. (1997) Complex Formation between Junctin, Triadin, Calsequestrin, and the Ryanodine Receptor. PROTEINS OF THE CARDIAC JUNCTIONAL SARCOPLASMIC RETICULUM MEMBRANE
10.1074/jbc.272.37.23389. *J. Biol. Chem.* 272, 23389-23397.
- Zolk, O., Schenke, C., and Sarikas, A. (2006) The ubiquitin-proteasome system: focus on the heart. *Cardiovasc Res* 70, 410-21.

8 Appendix

8.1 Aminoacid Table

Ala (A) Alanine	Leu (L) Leucine
Arg (R) Arginine	Lys (K) Lysine
Asn (N) Asparagine	Met (M) Methionine
Asp (D) Aspartic acid	Phe (F) Phenylalanine
Cys (C) Cysteine	Pro (P) Proline
Gln (Q) Glutamine	Ser (S) Serine
Glu (E) Glutamic acid	Thr (T) Threonine
Gly (G) Glycine	Trp (W) Tryptophan
His (H) Histidine	Tyr (Y) Tyrosine
Ile (I) Isoleucine	Val (V) Valine

8.2 Mass spectrometry supplementary data

1	PLQPAARPLP	PLCVRPASLV	HAATMSQAYS	SSQRVSSYRR	TFGGAPGFSL
51	GSPLSSPVFP	RAGFGTKGSS	SSMTSRVYQV	SRTSGGAGGL	GSLRSSRLGT
101	TRAPSYGAGE	LLDFSLADAV	NQEFLATRTN	EKVELQELND	RFANYIEKVR
151	FLEQQNAALA	AEVNRLKGRE	PTRVAELYEE	EMRELRRQVE	VLTNQRARVD
201	VERDNLIDDL	QRLKAKLQEE	IQLREEAENN	LAAFRADVDA	ATLARIDLER
251	RIESLNEEIA	FLKKVHEEEI	RELQAQLQEQ	QVQVEMDMSK	PDLTAALRDI
301	RAQYETIAAK	NISEAEEWYK	SKVSDLTQAA	NKNNDALRQA	KQEMMEYRHQ
351	IQSYTCEIDA	LKGTNDSLMR	QMRELEDRFA	SEANGYQDNI	ARLEEEIRHL
401	KDEMARHLRE	YQDLLNVKMA	LDVEIATYRK	LLEGEESRIN	LPIQTFSALN
451	FRETSPEQRG	SEVHTKKTVM	IKTIETRDGE	VVSEATQQQH	EVL

Table 8.1: Identificaion of desmin by peptide sequence.

Bold amino acids represent peptides that were detected in desmin (3% coverage).

#	b	b⁺⁺	b*	b^{*++}	b⁰	b⁰⁺⁺	Seq.
1	148.0757	74.5415					F
2	261.1598	131.0835					L
3	390.2023	195.6048			372.1918	186.5995	E
4	518.2609	259.6341	501.2344	251.1208	500.2504	250.6288	Q
5	646.3195	323.6634	629.2930	315.1501	628.3089	314.6581	Q
6	760.3624	380.6849	743.3359	372.1716	742.3519	371.6796	N
7	831.3995	416.2034	814.3730	407.6901	813.3890	407.1981	A
8	902.4367	451.7220	885.4101	443.2087	884.4261	442.7167	A
9	1015.5207	508.2640	998.4942	499.7507	997.5102	499.2587	L
10	1086.5578	543.7826	1069.5313	535.2693	1068.5473	534.7773	A
11	1157.5949	579.3011	1140.5684	570.7878	1139.5844	570.2958	A
12	1286.6375	643.8224	1269.6110	635.3091	1268.6270	634.8171	E
13	1385.7060	693.3566	1368.6794	684.8433	1367.6954	684.3513	V
14	1499.7489	750.3781	1482.7223	741.8648	1481.7383	741.3728	N
15							R

#	y	y⁺⁺	y*	y^{*++}	y⁰	y⁰⁺⁺	Seq.
15							F
14	1526.7921	763.8997	1509.7656	755.3864	1508.7816	754.8944	L
13	1413.7081	707.3577	1396.6815	698.8444	1395.6975	698.3524	E
12	1284.6655	642.8364	1267.6389	634.3231	1266.6549	633.8311	Q
11	1156.6069	578.8071	1139.5804	570.2938	1138.5963	569.8018	Q
10	1028.5483	514.7778	1011.5218	506.2645	1010.5378	505.7725	N
9	914.5054	457.7563	897.4789	449.2431	896.4948	448.7511	A
8	843.4683	422.2378	826.4417	413.7245	825.4577	413.2325	A
7	772.4312	386.7192	755.4046	378.2060	754.4206	377.7139	L
6	659.3471	330.1772	642.3206	321.6639	641.3365	321.1719	A
5	588.3100	294.6586	571.2835	286.1454	570.2994	285.6534	A
4	517.2729	259.1401	500.2463	250.6268	499.2623	250.1348	E
3	388.2303	194.6188	371.2037	186.1055			V
2	289.1619	145.0846	272.1353	136.5713			N
1	175.1190	88.0631	158.0924	79.5498			R

Table 8.2: Identification of amino acid sequence belonging to a peptid of desmin. Bold values represent matches with the amino acid sequence. Data is shown as m/z.

8.3 Tables

Tube	Geno- type	Sex	Age (wks)	Body weight (g)	Frozen tissue	VW (mg)	HW (mg)	VW/BW (mg/g)	HW/BW (mg/g)	Proteins $\mu\text{g}/\mu\text{l}$
1199	WT	f	3d	2.4	heart		14	5.9	5.9	1.9
1201	WT	f	3d	1.8	heart		9	5.0	5.0	1.2
1322	WT	f	3d	1.6	heart		11	7.1	7.1	1.4
1322	WT	f	3d	2.1	heart		14	6.5	6.5	1.1
1324	KO	f	3d	2.0	heart		11	5.4	5.4	1.9
1129	KO	f	4d	2.5	heart		23	9.3	9.3	2.8
1136	KO	f	4d	2.6	heart		16	6.1	6.1	1.3
1136	KO	f	4d	2.3	heart		14	6.1	6.1	2.4
1800	WT	m	2d	2.1	heart		10	4.9	4.9	1.7
1863	WT	m	3d	3.3	heart		16	4.9	4.9	1.7
1865	WT	m	3d	2.7	heart		14	5.1	5.1	1.2
1866	WT	m	3d	3.1	heart		17	5.5	5.5	1.7
1132	KO	m	2d	2.0	heart		13	6.5	6.5	1.4
1132	KO	m	2d	2.3	heart		15	6.6	6.6	1.7
1133	KO	m	2d	2.1	heart		18	8.7	8.7	1.5
1133	KO	m	2d	2.3	heart		25	11.1	11.1	2.1

Table 8.3: Raw data WT and KO NN.

Tube	Geno- type	Sex	Age (wks)	Body weight (g)	Frozen tissue	VW (mg)	HW (mg)	VW/BW (mg/g)	HW/BW (mg/g)	Proteins $\mu\text{g}/\mu\text{l}$
1473	WT	f	2	5.7	Ventricles	25	31	4.4	5.4	1.9
1102	WT	f	2	9.7	Ventricles	43	46	4.4	4.7	3.0
1103	WT	f	2	9.5	Ventricles	39	48	4.1	5.1	2.4
1532	WT	f	2	9.0	Ventricles	45	51	5.0	5.7	3.1
991	KO	f	2	6.5	Ventricles	48	57	7.4	8.8	4.5
942	KO	f	2	6.4	Ventricles	36	47	5.6	7.3	3.1
943	KO	f	2	7.0	Ventricles	48	55	6.9	7.9	4.0
944	KO	f	2	6.4	Ventricles	45	55	7.1	8.6	3.7
1101	WT	m	2	9.2	Ventricles	38	42	4.1	4.6	3.7
1470	WT	m	2	6.7	Ventricles	30	35	4.5	5.2	2.2
1471	WT	m	2	6.6	Ventricles	35	39	5.3	5.9	2.5
1472	WT	m	2	7.5	Ventricles	42	54	5.6	7.2	3.9
938	KO	m	2	6.6	Ventricles	49	56	7.4	8.5	4.2
939	KO	m	2	7.0	Ventricles	54	60	7.7	8.6	4.0
940	KO	m	2	6.8	Ventricles	45	52	6.6	7.7	3.2
941	KO	m	2	6.9	Ventricles	41	50	5.9	7.2	3.7

Table 8.4: Raw data WT and KO 2wks.

Tube	Geno- type	Sex	Age (wks)	Body weight (g)	Frozen tissue	VW (mg)	HW (mg)	VW/BW (mg/g)	HW/BW (mg/g)	Proteins $\mu\text{g}/\mu\text{l}$
973	WT	f	4	13.6	Ventricles	63	71	4.6	5.2	1.8
974	WT	f	4	12.9	Ventricles	58	63	4.5	4.9	2.3
975	WT	f	4	14.7	Ventricles	66	71	4.5	4.8	3.5
976	WT	f	4	16.1	Ventricles	72	77	4.5	4.8	2.1
903	KO	f	4	16.1	Ventricles	93	98	5.8	6.1	2.6
904	KO	f	4	18.4	Ventricles	105	115	5.7	6.2	2.4
905	KO	f	4	16.5	Ventricles	89	103	5.4	6.2	2.8
906	KO	f	4	19.5	Ventricles	114	125	5.8	6.4	2.2
932	WT	m	4	19.0	Ventricles	82	91	4.3	4.8	3.1
933	WT	m	4	16.9	Ventricles	77	83	4.5	4.9	2.9
934	WT	m	4	14.8	Ventricles	71	83	4.8	5.6	2.5
935	WT	m	4	16.9	Ventricles	69	81	4.1	4.8	2.2
907	KO	m	4	17.4	Ventricles	102	112	5.9	6.5	3.5
908	KO	m	4	21.4	Ventricles	113	126	5.3	5.9	4.0
936	KO	m	4	18.9	Ventricles	106	111	5.6	5.9	2.6
937	KO	m	4	18.4	Ventricles	111	126	6.0	6.8	2.6

Table 8.5: Raw data WT and KO 4wks.

Tube	Geno- type	Sex	Age (wks)	Body weight (g)	Frozen tissue	VW (mg)	HW (mg)	VW/BW (mg/g)	HW/BW (mg/g)	Proteins $\mu\text{g}/\mu\text{l}$
1156	WT	f	6	17.9	Ventricles	82	87	4.6	4.9	3.3
1307	WT	f	6	17.7	Ventricles	87	99	4.9	5.6	4.2
1308	WT	f	6	18.1	Ventricles	83	95	4.6	5.2	2.6
1309	WT	f	6	19.1	Ventricles	91	100	4.8	5.2	4.2
1053	KO	f	6	16.2	Ventricles	95	104	5.9	6.4	2.2
1054	KO	f	6	16.3	Ventricles	100	109	6.2	6.7	4.0
1055	KO	f	6	17.0	Ventricles	147	160	8.6	9.4	6.5
1056	KO	f	6	17.6	Ventricles	99	109	5.6	6.2	4.2
1022	WT	m	6	24.4	Ventricles	116	126	4.7	5.2	3.0
1023	WT	m	6	24.0	Ventricles	112	119	4.7	5.0	4.6
1155	WT	m	6	20.8	Ventricles	98	108	4.7	5.2	4.0
1157	WT	m	6	23.7	Ventricles	105	122	4.4	5.1	3.2
1050	KO	m	6	24.2	Ventricles	151	176	6.2	7.3	6.8
1051	KO	m	6	22.1	Ventricles	137	154	6.2	7.0	5.5
1052	KO	m	6	22.1	Ventricles	134	142	6.1	6.4	5.0
1140	KO	m	6	23.5	Ventricles	147	173	6.3	7.4	1.3

Table 8.6: Raw data WT and KO 6wks.

Tube	Geno- type	Sex	Age (wks)	Body weight (g)	Frozen tissue	VW (mg)	HW (mg)	VW/BW (mg/g)	HW/BW (mg/g)	Proteins $\mu\text{g}/\mu\text{l}$
1364	WT	f	9	18.7	Ventricles	102	116	5.5	6.2	2.8
1400	WT	f	9	20.8	Ventricles	101	107	4.9	5.1	3.7
1403	WT	f	9	20.5	Ventricles	90	97	4.4	4.7	2.0
1407	WT	f	9	21.6	Ventricles	86	100	4.0	4.6	2.2
1030	KO	f	9	19.8	Ventricles	127	140	6.4	7.1	2.8
1031	KO	f	9	20.0	Ventricles	118	130	5.9	6.5	2.6
1398	KO	f	9	22.8	Ventricles	137	148	6.0	6.5	4.8
1399	KO	f	9	23.4	Ventricles	137	143	5.9	6.1	3.5
1024	WT	m	9	25.9	Ventricles	119	132	4.6	5.1	3.5
1025	WT	m	9	24.1	Ventricles	107	128	4.4	5.3	1.7
1026	WT	m	9	24.2	Ventricles	104	118	4.3	4.9	4.2
1027	WT	m	9	24.0	Ventricles	120	134	5.0	5.6	2.5
1028	KO	m	9	28.0	Ventricles	175	193	6.3	6.9	4.3
1029	KO	m	9	25.8	Ventricles	150	186	5.8	7.2	2.2
1310	KO	m	9	26.9	Ventricles	188	204	7.0	7.6	4.7
1311	KO	m	9	25.8	Ventricles	182	198	7.1	7.7	2.9

Table 8.7: Raw data WT and KO 9wks.

Tube	Geno- type	Sex	Age (wks)	Body weight (g)	Frozen tissue	VW (mg)	HW (mg)	VW/BW (mg/g)	HW/BW (mg/g)	Proteins $\mu\text{g}/\mu\text{l}$
1712	WT	f	13	23.3	Ventricles	103	109	4.4	4.7	4.2
1791	WT	f	13	19.4	Ventricles	76	82	3.9	4.2	3.2
1792	WT	f	13	16.8	Ventricles	78	80	4.6	4.8	2.1
1793	WT	f	13	21.6	Ventricles	92	96	4.3	4.4	2.5
1477	KO	f	13	22.5	Ventricles	139	157	6.2	7.0	4.6
1478	KO	f	13	20.4	Ventricles	136	152	6.7	7.5	4.6
1479	KO	f	13	20.8	Ventricles	147	157	7.1	7.5	5.3
1480	KO	f	13	23.6	Ventricles	153	164	6.5	6.9	5.6
1334	WT	m	13	25.9	Ventricles	118	125	4.6	4.8	3.8
1335	WT	m	13	31.0	Ventricles	158	174	5.1	5.6	4.1
1336	WT	m	13	27.6	Ventricles	135	147	4.9	5.3	4.0
1337	WT	m	13	24.3	Ventricles	115	132	4.7	5.4	4.7
1481	KO	m	13	29.2	Ventricles	201	218	6.9	7.5	6.2
1474	KO	m	13	31.7	Ventricles	230	258	7.3	8.1	7.3
1475	KO	m	13	27.3	Ventricles	222	241	8.1	8.8	6.0
1476	KO	m	13	31.3	Ventricles	206	214	6.6	6.8	6.6

Table 8.8: Raw data WT and KO 13wks.

Tube	Geno- type	Sex	Age (wks)	Body weight (g)	Frozen tissue	VW (mg)	HW (mg)	VW/BW (mg/g)	HW/BW (mg/g)	Proteins $\mu\text{g}/\mu\text{l}$
1626	WT	f	52	38.0	Ventricles	126	145	3.3	3.8	3.3
1628	WT	f	50	29.2	Ventricles	126	137	4.3	4.7	4.3
1629	WT	f	50	29.3	Ventricles	117	122	4.0	4.2	4.2
1915	WT	f	50	30.3	Ventricles	106	116	3.5	3.8	2.9
2004	WT	f	51	26.9	Ventricles	169	195	6.3	7.3	3.9
2005	WT	f	51	22.1	Ventricles	84	100	3.8	4.5	3.6
1717	WT	f	50	31.5	Ventricles	172	193	5.5	6.1	3.6
1979	WT	f	51	33.8	Ventricles	288	418	8.5	12.4	2.8
1624	KO	m	52	32.2	Ventricles	130	142	4.0	4.4	3.0
1625	KO	m	52	36.6	Ventricles	141	146	3.9	4.0	5.0
1627	KO	m	50	33.9	Ventricles	148	157	4.4	4.6	4.1
1788	KO	m	50	30.5	Ventricles	145	156	4.8	5.1	3.9
1623	KO	m	48	42.1	Ventricles	260	288	6.2	6.8	5.7
1641	KO	m	53	39.4	Ventricles	256	276	6.5	7.0	5.3
1913	KO	m	52	42.2	Ventricles	226	249	5.4	5.9	4.5
1914	KO	m	50	31.5	Ventricles	205	226	6.5	7.2	6.5

Table 8.9: Raw data WT and KO 50wks.

8.4 List of abbreviations

A	Ampere
AMP	Adenosine monophosphate
AMC	7-Amino-4-methylcoumarin
APS	Ammonium persulphate
ATP	Adenosine triphosphate
AU	Arbitrary unit
B	Beta
bp	Base pair(s)
BSA	Bovine serum albumin
BW	Body weight
$^{\circ}\text{C}$	Degree Celsius
cMyBP-C	Cardiac Myosin-binding protein-C
Cry	Crystallin
CSQ	Calsequestrin
Da	Dalton
DMSO	Dimethyl sulfoxide

DNA	Deoxyribonucleic acid
DRM	Desmin related myopathy
DTT	Dithiothreitol
DUB	De-ubiquitinating enzyme
ECL	Enhanced chemiluminescence
EDTA	Ethylene diamine tetraacetic acid
e.g.	<i>exempli gratia</i> (for example)
<i>et al.</i>	<i>et alii</i> (and others)
FHC	Familial hypertrophic cardiomyopathy
g	Gram
h	Hour
HCM	Hypertrophic cardiomyopathy
Hsp	Heat shock protein
HW	Heart weight
Hz	Hertz
i.e.	<i>id est</i> (that is)
IgG	Immunoglobulin G
Inc.	Incorporation
kDa	Kilo Dalton
KO	Knock-out
l	Liter
LV	Left ventricle
m	Milli- (1×10^{-3})
M	Molar
mA	Milliampere
Maldi	Matrix Assisted Laser Desorption/ Ionisation
mg	Milligram
min	Minutes
ml	Milliliter
mM	Millimolar
MW	Molecular weight
mRNA	Messenger ribonucleic acid
MyBP-C	Myosin-binding protein-C
MHC	Myosin heavy chain

m/z	Mass-to-charge-ratio
μ	Micro (1 x 10 ⁻⁶)
μg	Microgram
μl	Microliter
μM	Micromolar
N	Amino-
NaF	Sodium fluoride
NaOH	Sodium hydroxide
NF	Necrosis factor
NIH	National Institutes of Health
nm	Nanometer
NN	Neonates
no.	Number
pACC	Phosphorylated acetyl-CoA carboxylase
P	Phosphate
PAGE	Polyacrylamide gel electrophoresis
PBS	Phosphate buffered saline
RNA	Ribonucleic acid
RIPA	Radio Immuno Precipitation Assay
rpm	Rotation per minute
RT	Room temperature
S	Svedberg
SDS	Sodium dodecyl sulfate
sec	Seconds
SEM	Standard error of mean
SR	Sarcoplasmic reticulum
TAC	Transverse aortic constriction
TBS	Tris buffered saline
TBS-T	Tris buffered saline with tween-20
TEMED	N. N. N'. N'-Tetramethylethylenediamine
TOF	Time-of-flight
UPS	Ubiquitin-proteasome system
wks	Weeks
WT	Wild type

9 Acknowledgement

I want to thank Prof. Dr. Thomas Eschenhagen for the friendly supervision. The great sustain made many things easier, especially before the congress of Mannheim and in the last phases of my thesis. I am still amazed, how quick emails were answered.

I would like to express my sincere gratitude to Dr. Lucie Carrier for the wonderful supervision and the straight forward motivation over the whole time of my thesis. I am very thankful for the support in moments of complete disappointment.

Many thanks go to the staff members of the institute for the friendly and helpful atmosphere. Especially to Saskia Schlossarek for the assistance with the chymotrypsin-like activity, to Giulia Mearini for the supervision of the immunoprecipitations, to Denise Jühr who made me run around the lake Außenalster in 33min, to Dr. Felix Friedrich for the organization of the soccer team of the laboratory and to Lisa Krämer who had always a smile on the face for me when I came with a problem.

I wish to thank my friend Bojan Pounarov, who found the perfect words over the years to push me forward in the best and worst moments of my life.

Special thanks go to my Natalie Hietsch, who knew how to fill the little time we had with love.

Finally and especially, I wish to thank my parents: My mother for giving me her enthusiasm and the positive attitude to life. My father for giving me the ambition and the proof-reading of my abstracts. They both supported and believed in me my entire life.

10 Curriculum Vitae

Personal data:

First names: Daniel Riccardo

Last name: Englmann

Date of birth: 03.06.1981

City of birth: Tübingen

Education:

1987-2000 Schickhardt-Secondary School Stuttgart
05.06.2000 Abitur
10.02-05.09 Study of medicine at the University of Hamburg
01.08.2004 1. medical examination
05.05.2009 2. medical examination
06.02-08.02 Nursery clerkship at the Hospital of Udine/ Italy
10.05-05.06 Erasmus: University of Valladolid/ Spain
02.08-05.08 Internship at the University of Bern/ Switzerland.
Hospital of Lugano
06.08-09.08 Internship at the University of Cape Town/
Southafrica. Victoria and Jooste Hospital
Since 06.06 Medical doctoral student
at the Institute of Experimental and
Clinical Pharmacology and Toxicology.
University Medical Center Hamburg-Eppendorf

Work experience:

06.00-04.02 Rescue Service of the German Red Cross

11 Declaration

I declare that the work reported in the dissertation submitted to the University of Hamburg and entitled

Alterations of the ubiquitin-proteasome system in targeted cMyBP-C mice with
hypertrophic cardiomyopathy

was realized in person in the Institute of Experimental and Clinical Pharmacology and Toxicology under the supervision of Prof. Dr. Thomas Eschenhagen. All sources of information as well as the results obtained in collaboration with other people are pointed out.

The dissertation has not been submitted in whole or in part for a degree at any other university.

Hamburg, May 2009

Daniel Riccardo Englmann